# CD109 on dendritic cells regulates airway hyperreactivity and eosinophilic airway inflammation

# CD109 on dendritic cells regulates airway hyperreactivity and eosinophilic airway inflammation

Yuya Aono, MD,[a] Yuzo Suzuki, MD, PhD,[a] Ryo Horiguchi, PhD,[b] Yusuke Inoue, MD, PhD,[a] Masato Karayama, MD, PhD,[a] Hironao Hozumi, MD, PhD,[a] Kazuki Furuhashi, MD, PhD,[a] Noriyuki Enomoto, MD, PhD,[a] Tomoyuki Fujisawa, MD, PhD,[a] Yutaro Nakamura, MD, PhD,[a] Naoki Inui, MD, PhD,[a] Shinji Mii, MD, PhD,[c] Masahide Takahashi, MD, PhD,[c,d] Takafumi Suda, MD, PhD[a]

[a]Second Division, Department of Internal Medicine, Hamamatsu University School of Medicine, Hamamatsu, Japan

[b]Advanced Research Facilities and Services, Hamamatsu University School of Medicine

[c]Department of Pathology, Nagoya University Graduate School of Medicine, Nagoya, Japan.

[d]International Center for Cell and Gene Therapy, Fujita Health University, Toyoake, Japan

**Corresponding author:**

Yuzo Suzuki, PhD

1-20-1, Handayama, Higashi-ku, Hamamatsu, Shizuoka, Japan, 431-3192

**Phone:** +81-53-435-2263

**Fax:** +81-53-435-2354

**E-mail:** yuzosuzu@hama-med.c.jp

**Running Title**: CD109 on DCs regulates asthma

**Funding**: This work was supported by a grant-in-aid for scientific research (19K17632 and 22K08279 to YS) from the Japan Society for the Promotion of Science, the Basic Research Support Program from Japan Society of Allergology (YS), Japan Allergy Foundation (YS)



AJRCMB Articles in Press. Published October 10, 2022 as 10.1165/rcmb.2022-0109OC

and a HUSM grant-in-aid from the Hamamatsu University School of Medicine (42351E-1013511 to YA and 42351E-101337 and 65002-711441to YS).

**Conflicts of interest**: YA, YS and TS equally have Japanese patent application No.2022-036500. The other authors declare no competing interests.

## ACKNOWLEDGMENTS

YA, YS and TS equally have Japanese patent application No.2022-036500. The other authors declare no competing interests. The studies described in this article were financially supported by a grant-in-aid for scientific research from the Japan Society for the Promotion of Science (19K17632 and 22K08279 to YS), the Basic Research Support Program from Japan Society of Allergology (YS), Japan Allergy Foundation (YS), and a HUSM grant-in-aid from the Hamamatsu University School of Medicine (42351E-1013511 to YA and 42351E-101337 and 65002-711441to YS).

We thank Enago for editing a draft of the manuscript.

## Author contribution

Y. A. and Y. S. designed the research and performed experiments, analyzed data, and wrote the paper; R.H., Y. I., M. K., H. H, K. F., N. E., T. F., Y. N., and N. I. analyzed data; S. M., and N. T. designed the research and analyzed data; T. S. designed the research and wrote the paper.

**This article has an online data supplement, which is accessible from this issue's table of content online at www.atsjournals.org.**



AJRCMB Articles in Press. Published October 10, 2022 as 10.1165/rcmb.2022-0109OC

**Abstract**

Asthma is a chronic airway inflammatory disease characterized by airway hyperreactivity (AHR) and eosinophilic airway inflammation. Dendritic cells (DCs) are essential for the development of asthma via presenting allergens, causing Th2 skewing and eosinophil inflammation. Recent studies have revealed that CD109, a glycosylphosphatidylinositol-anchored glycoprotein, is involved in the pathogenesis of inflammatory diseases such as rheumatoid arthritis and psoriasis. However, no study has addressed the role of CD109 in asthma. This study sought to address the role of CD109 on DCs in the development of AHR and allergic inflammation. CD109 deficient mice (*CD109*$^{-/-}$ mice) were sensitized with house dust mite (HDM) or ovalbumin and compared to wild-type (WT) mice for induction of AHR and allergic inflammation. CD109-deficient mice had reduced AHR and eosinophilic inflammation together with lower Th2 cytokine expression compared to WT mice. Interestingly, CD109 expression was induced in lung conventional DC2s (cDC2s), but not lung cDC1s, upon allergic challenge. Lung cDC2s from *CD109*$^{-/-}$ mice had a poor ability to induce cytokine production in *ex vivo* DC-T cell cocultures with high expression of RUNX3, resulting in suppression of Th2 differentiation. Adoptive transfer of bone-marrow-derived *CD109*$^{-/-}$ DCs loaded with HDM failed to develop AHR and eosinophilic inflammation. Finally, administration of monoclonal anti-CD109 antibody reduced airway eosinophils and significantly decreased AHR. Our results suggest the involvement of CD109 in asthma pathogenesis. CD109 is a novel therapeutic target for asthma.

**Key words:** Asthma; CD109; dendritic cell; airway hyperreactivity; eosinophil inflammation.

**Abbreviations:**

| | |
|---|---|
| AHR | Airway hyperreactivity |



AJRCMB Articles in Press. Published October 10, 2022 as 10.1165/rcmb.2022-0109OC

| | |
|---|---|
| ALK1 | Activin receptor-like kinase1 |
| BAL | Bronchoalveolar lavage |
| BMDCs | bone-marrow-derived DCs |
| $C_{dyn}$ | Dynamic compliance |
| DCs | Dendritic cells |
| GRP | Glucose-regulated protein |
| HDM | House dust mite |
| ICOS-L | Inducible costimulatory ligand |
| IFN-γ | Interferon-γ |
| IL-2/4/5/6/13/17A | Interleukin-2/4/5/6/13/17A |
| ILC2s | Type 2 innate lymphocyte cells |
| JAK | Janus kinase |
| OVA | Ovalbumin |
| PBMC | Peripheral blood mononuclear cells |
| PBS | Phosphate-buffered saline |
| PD-L1/2 | Programmed death ligand-1/2 |
| $R_L$ | Lung resistance |
| RUNX3 | Runt-related transcription factor 3 |
| TCC | Total cell counts |
| TGF-β | Transforming growth factor-β |
| Th2 | T-helper type 2 |
| TNF-α | Tumor necrosis factor |
| TSLP | Thymic stromal lymphoprotein |
| WT | Wild type |



AJRCMB Articles in Press. Published October 10, 2022 as 10.1165/rcmb.2022-0109OC

## INTRODUCTION

Asthma, a chronic respiratory disease characterized by airway hyperreactivity (AHR) and eosinophilic airway inflammation. (1-4) Accumulated evidence has shown that asthma is composed of heterogenous phenotypes where immune cells are complexity involved. Allergic sensitization in which dendritic cells (DCs) presents allergens, followed by T-helper type 2 (Th2) cell skewing and eosinophilic inflammation plays a critical role in allergic asthma. DCs interact with Group 2 innate lymphocyte cells (ILC2s) to initiate allergic inflammation in non-allergic asthma (5, 6), indicating essential roles of DCs in development of both allergic and non-allergic asthma.

CD109, a glycosylphosphatidylinositol (GPI)-anchored glycoprotein cell-surface antigen, is a member of the alpha2-macroglobulin/C3, C4, C5 family of thioester-containing proteins. (7, 8) Its primary function is downregulating transforming growth factor (TGF)-β signaling by binding to TGF-β receptor I, (9) TGF-β,(10) activin receptor-like kinase1 (ALK1), (11) and 78-kDa glucose-regulated protein (GRP78).(12) CD109 is expressed on the several types of cancers and is involved in disease progression. Indeed, CD109 expression is associated with poor prognosis in cancer. (13-18) More recently, CD109 is reported to be involved in the pathogenesis of inflammatory disease in a murine model of rheumatoid arthritis(19) and psoriasiform inflammation. (20) However, studies investigating CD109 involvement in allergic inflammation are lacking.

We investigated the role of CD109 on DCs in the pathogenesis of asthma. We showed a critical role for CD109 on DCs in the development of AHR and eosinophilic inflammation using a murine model of allergic asthma. Further, blockade of CD109



AJRCMB Articles in Press. Published October 10, 2022 as 10.1165/rcmb.2022-0109OC

ameliorated AHR and eosinophilic inflammation. This study provides new evidence for an underlying role of CD109 on DCs in asthma pathogenesis, which can be a novel therapeutic target.

**Materials and methods**

Detailed methodology was described in the **Supplementary Method** section

***Mice***

Female C57BL/6 mice, *CD109*$^{-/-}$ mice (8 to 10-weeks-old) and OVA-specific T cell receptor (TCR) transgenic mice (OT-II) were used. *CD109*$^{-/-}$ mice were generated as previously described. (21) All experimental protocols were approved by the Institutional Animal Care and Use Committee of Hamamatsu University School of Medicine (29-045).

***AHR induction and measurement of airway hyperresponsiveness***

Mice were intranasally (i.n.) sensitized with 50 μg HDM (*Dermatophagoides. pteronyssinus*; Greer Laboratories) on day 1, followed by 10 μg HDM (i.n.) on days 8 and 13. In some experiments, mice were treated with neutralizing monoclonal anti-mouse CD109 antibody (i.n., 100 μg/mouse, Abmart) or IgG isotype controls (Fujifilm). In the OVA model, mice were intraperitoneally immunized with OVA (50 μg, Sigma-Aldrich) and Alum (2 mg, Thermo Fischer Scientific) on days 1 and 8, and subsequently intranasally challenged with 50 μg OVA on days 19 to 21.

Two days after the last HDM challenge or one day after the last OVA challenge, airway resistance and dynamic compliance measurements were conducted using the Fine Pointe RC system (Buxco Electronics, Inc), as previously described. (22-24) After measuring AHR, BAL cells, serum, lung histological sections and lung lysates were obtained and quantified.



AJRCMB Articles in Press. Published October 10, 2022 as 10.1165/rcmb.2022-0109OC

***Identification of lung DC subsets***

Lung DCs were defined as lacking the classical lineage markers (CD3 ε , NK1.1, CD19, CD45R) and $CD45^+$ $CD64^-$ F4/80$^-$ I-A/I-$E^+$ $CD11c^+$ cells. Lung DC subsets were then identified based on XCR1 and CD172a expression (cDC1; $XCR1^+$ $CD172a^-$ and cDC2; $XCR1^-$ $CD172a^+$).(25-28)

***Capability of antigen uptake and T cell proliferation of lung DC subsets***

Alexa Fluor 647-labeled OVA (Thermo Fisher Scientific) was intranasally administered in the last challenge to assess capability of antigen uptake and-presentation of lung DCs.

***In vitro coculture of lung DC subset and $CD4^+$ T cells***

Purified naïve $CD4^+$ T cells ($2 \times 10^5$/ml) obtained from OT-II murine spleen were cocultured with lung DC subsets ($2 \times 10^4$/ml) for 7 days in the presence of 10 μg/ml $OVA_{323-339}$ peptide (Invitrogen). Cytokine in the coculture supernatants, apoptosis and proliferation for cocultured $CD4^+$ T cells were examined.

***Gene expression analysis***

The difference in transcript abundance between lung DC subsets purified from HDM-sensitized *CD109*$^{-/-}$ mice or WT mice was analyzed using the nCounter Immunology Panel (NanoString Technologies, Inc.). Heat plots were generated using nSolver software.

***Preparation of bone marrow-derived DCs and adoptive transfers***

HDM-loaded BMDCs ($2.0 \times 10^5$) were adoptively transferred intravenously into C57BL/6 mice (day 1), and subsequently challenged intratracheally with HDM-loaded BMDCs ($2.0 \times 10^5$) or HDM (10 μg/mouse) on days 8 and 13 and sacrificed on day 15.



AJRCMB Articles in Press. Published October 10, 2022 as 10.1165/rcmb.2022-0109OC

***Flow cytometry analysis***

Flow cytometry was done with a Gallios Flow Cytometer (Beckman Coulter). Data were analyzed with FlowJo version 8.6 software (TreeStar).

***Reverse transcription-polymerase chain reaction (RT-PCR) assays***

Relative gene expression levels were measured by using RT-PCR.

***Statistical analysis***

Student's t-test and one-way ANOVA post hoc test with Tukey's multiple comparison test were used for comparisons. A P-value < 0.05 was significant. All data are means ± SEM. Statistical analyses were performed using GraphPad Prism version 6 (GraphPad Software).

**RESULTS**

***Lack of CD109 ameliorated airway hyperreactivity and eosinophilic airway inflammation.***

To investigate a role of CD109 in development of AHR and eosinophilic inflammation, *CD109*$^{-/-}$ and wild-type (WT) mice were sensitized and intranasally challenged with house dust mite extract (HDM) (**Fig. 1A**). Two days after the challenge, lung function was evaluated via direct measurements of lung resistance ($R_L$) and dynamic compliance ($C_{dyn}$). HDM-challenged *CD109*$^{-/-}$ mice had significantly decreased AHR, representing lower lung resistance and higher dynamic compliance than HDM-challenged WT mice (**Fig. 1B**). HDM-challenged *CD109*$^{-/-}$ mice had significantly lower number of eosinophils in BAL than WT mice (**Fig. 1C**). Meanwhile, total cell counts were not different between HDM-challenged WT mice, and number of macrophages and lymphocytes were rather increased in HDM-challenged *CD109*$^{-/-}$ mice. There were some differences in BAL cells between PBS-treated



AJRCMB Articles in Press. Published October 10, 2022 as 10.1165/rcmb.2022-0109OC

*CD109*$^{-/-}$ mice and PBS-treated WT mice. PBS-treated *CD109*$^{-/-}$ mice tended to have higher number of total cells, lymphocytes and neutrophils together with decreased macrophages in BAL compared with PBS-treated WT mice, but these differences were not statistically significant. Histological analysis revealed decreased bronchial wall thickening, peribronchiolar cell infiltration, and a lower number of periodic acid-Schiff $(PAS)^+$ cells in HDM-challenged *CD109*$^{-/-}$ mice, compared with those observed in HDM-challenged WT mice (**Fig. 1D**). Consistent with these observations, a significant reduction in expression of IL-4, IL-5, IL-13, and IL-33 in the lungs and HDM-specific IgE in sera were ~~was~~ observed in *CD109*$^{-/-}$ mice, compared with those observed in HDM-challenged WT mice. (**Figs. 1E and 1F**). The frequencies of ILC2s and Th2 cells expressing IL-5 or IL-13 were also decreased in *CD109*$^{-/-}$ mice (**Fig. S1**). These observations of an attenuated asthmatic phenotype, including AHR, eosinophilic airway inflammation, and lung histology, were also found in *CD109*$^{-/-}$ mice in an ovalbumin (OVA)-challenged asthma model (**Fig. S2**).

***CD109 expression was induced by allergen challenge in WT mice.***

We examined types of immune cells expressing CD109 in the lungs of the asthma model. In a steady state, no immune cells expressed CD109 in the lung. In OVA-challenged mice, CD109 expression was induced in cDC2s, B cells, and ILC2s but not in lung cDC1s (**Fig. 2A**). Similarly, increased CD109 expression on cDC2s and ILC2s were found with HDM-challenged mice (**Fig. S3**). Phenotypically, lung DCs with CD109 expression had increased PD-L1, ICOS-L, and CD80 expression, while CD86 expression was decreased, compared with those without CD109 expression (**Fig. 2C**).

***Lung cDC2s from CD109$^{-/-}$ mice had poor capacity of antigen presentation, and showed impaired cytokine production in ex vivo coculture with naïve T cells.***



AJRCMB Articles in Press. Published October 10, 2022 as 10.1165/rcmb.2022-0109OC

Since CD109 was inducible exclusively in lung cDC2s, but not in lung cDC1s, we next investigated whether lung cDC2s from *CD109*$^{-/-}$ mice altered their function in terms of Th responses. Previous studies showed distinct function of lung DC subsets in immune reaction. (25-27, 29-31) Especially, cDC2s were reported to preferentially induce Th2 polarization at a steady state. (31-34) Lung cDC2s were purified from OVA-challenged *CD109*$^{-/-}$ and WT mice (**Figs. 3A and 3B**). Subsequently, lung cDC2s were cocultured with naïve CD4$^+$ T cells isolated from OT-II mice in the presence of $OVA_{323–339}$ peptide. In coculture supernatants with lung cDC2s from WT mice, large amounts of IL-2, IL-6, IL-13, IL-17A, TNF-α, and IFN-γ were detected. Comparing lung cDC2s from *CD109*$^{-/-}$ mice and those from WT mice, the concentration of IL-13 in the cocultures with *CD109*$^{-/-}$ lung cDC2s was significantly lower than those with WT lung-cDC2s (**Fig. 3C**). The levels of IL-6, IL-17A, TNF-α, and IFN-γ were also significantly decreased in cocultures with lung cDC2s from *CD109*$^{-/-}$ mice, compared with those with lung cDC2s from WT mice. To explore the distinct capability of lung DCs from *CD109*$^{-/-}$ mice on proliferation and apoptosis of cocultured CD4$^+$ T cells, the cocultured cells were stained with cell trace assay or annexin V and propidium iodide, respectively. The proliferation was significantly reduced naïve OT-II CD4$^+$ T cells cocultured with *CD109*$^{-/-}$ lung cDC2s, compared with in those with WT lung cDC2s (**Fig. 3D**). In addition, the cell death was significantly increased in naïve OT-II CD4$^+$ T cells cocultured with *CD109*$^{-/-}$ lung cDC2s, compared with in those with WT lung cDC2s (**Fig. 3E**).

Because antigen uptake and presentation are known as essential for DCs mediated T cell differentiation, mice were challenged with fluoresceine-labeled OVA on day20 under protocol of **Fig. 3A**. The fluoresceine level of *CD109*$^{-/-}$ lung cDC2s were significantly lower than those of WT lung-cDC2s (**Fig. 3F**). Collectively, these results suggest that lung cDC2s from *CD109*$^{-/-}$ mice had poor capability on antigen presentation.



AJRCMB Articles in Press. Published October 10, 2022 as 10.1165/rcmb.2022-0109OC

***CD109 expression in DCs was responsible for asthmatic phenotype induction during allergen sensitization and allergen challenge***

Because we found that lung cDC2s from *CD109*$^{-/-}$ mice impaired the induction of several cytokines, including IL-13, in cocultures with naïve T cells, we examined whether the absence of CD109 in DCs are directly responsible for attenuating AHR and eosinophilic airway inflammation. To study the role of CD109 in DC function during allergen sensitization phase, WT mice were intravenously adoptive transferred HDM-loaded bone-marrow-derived DCs (BMDCs) from either *CD109*$^{-/-}$ or WT mice, and challenged with HDM (**Fig. 4A)**. This asthma model showed an increase of AHR, eosinophilic airway inflammation, and characteristic pathologic features of asthma using HDM-loaded WT BMDCs (**Figs. 4B, 4C, and 4D**). However, AHR and the number of eosinophils, macrophages and lymphocytes in BAL were significantly lower in mice sensitized with HDM-loaded *CD109*$^{-/-}$ BMDCs than those sensitized with WT BMDCs (**Figs. 4B and 4C**). Histological analysis showed decreased bronchial wall thickening and inflammatory cells, together with reduced number of PAS$^{+}$ cells in *CD109*$^{-/-}$ BMDC-sensitized mice, compared with WT BMDC-sensitized mice (**Fig. 4D**).

Previous study showed that depletion of lung CD11c$^{+}$ cells during allergen challenge abrogate characteristic features of asthma, indicating DCs also play roles during allergic challenge phase to induce allergic inflammation (35). To clarify whether CD109 on lung DCs is involved in the challenge phase of asthmatic inflammation, WT mice were intravenously immunized same as in **Fig. 4**, and subsequently intratracheally challenged with HDM-loaded BMDCs from either *CD109*$^{-/-}$ or WT mice (**Fig. S4A**). Mice challenged with HDM-loaded *CD109*$^{-/-}$ BMDCs showed significantly decreased AHR and reduced number of eosinophils in BAL than those with WT BMDCs (**Figs. S4B** and **S4C**). Consistently,



AJRCMB Articles in Press. Published October 10, 2022 as 10.1165/rcmb.2022-0109OC

reduced bronchial wall thickening, peribronchiolar inflammation and $PAS^+$ cells were observed in *CD109*$^{-/-}$ BMDC-challenged mice, compared with WT BMDC-challenged mice (**Fig. S4D**).

***Gene expression analyses in lung cDCs from CD109*$^{-/-}$ *mice***

Because the functional difference in the induced cytokine productions was noted between lung cDC2s between *CD109*$^{-/-}$and WT mice, we next analyzed gene expression profiles in lung cDC2 from *CD109*$^{-/-}$ and WT mice using Nanostring technology. Lung cDC2s from *CD109*$^{-/-}$ mice showed decreased eotaxin (*Ccl24* and *Ccl26*) and Th2-related cytokine (*Il4*, *Il5*, *Il13*, and *Il33*) expression and increased Th1-related cytokine (*Il18*, *Il12*, and *Cxcl9*), compared those from WT mice (**Fig. 5A**). Notably, among transcription factors, lung cDC2s from *CD109*$^{-/-}$ mice increased *Runx3* expression together with decreased *Rorc* expression compared those from WT mice. Recent studies show distinct phenotypes of cDC2 populations (cDC2a, an anti-inflammatory phenotype and cDC2b, a pro-inflammatory phenotype) based on transcription factors. (26, 27) RUNX3 is a characteristic transcription factor of the anti-inflammatory cDC2a phenotype. (26) Consistent with array data, lung cDC2s from *CD109*$^{-/-}$ mice increased expression of RUNX3 protein than those from WT mice (**Fig. 5B**). Additionally, CD109 is known to negatively regulate TGF-β signaling, where RUNX3 corporate the intracellular signal transducers, SMAD2 and SMAD3. (8) Thus, we examined phosphorylated SMAD2/3, indicating that phosphorylated SMAD2/3 was increased in lung cDC2s from *CD109*$^{-/-}$ mice than those from WT mice (**Figs. 5C and S5**).

***Anti-CD109 monoclonal antibody ameliorated AHR and eosinophilic airway inflammation during both allergen sensitization and allergen challenge.***



AJRCMB Articles in Press. Published October 10, 2022 as 10.1165/rcmb.2022-0109OC

Finally, we hypothesized that CD109 blockade could be a novel therapeutic strategy for asthma. To address this, we examined whether anti-CD109 monoclonal antibody (mAb) treatments during either allergen sensitization or allergen challenge phases reduced AHR and eosinophilic airway inflammation in HDM-challenged mice, respectively. To examine efficacy of anti-CD109 mAb during allergen sensitization phase, WT mice were intranasally administered anti-CD109 mAb or isotype IgG one day before HDM sensitization, and then mice were sensitized and challenged with HDM (**Fig. 6A**). Mice treated with anti-CD109 mAb showed significantly reduced AHR and eosinophils counts in BAL (**Fig. 6B** and **6C**). Histological analyses also revealed reduced airway inflammation and $PAS^+$ cells in anti-CD109 mAb-administered mice (**Fig. 6D**). The levels of IgE, HDM-specific IgE, and IgG1 did not significantly differ (data not shown).

Next, we evaluated effects of anti-CD109 mAb during allergen challenge phase. WT mice were intranasally immunized with HDM, and then anti-CD109 mAb or isotype IgG was administered intranasally on days 7 and 12 (**Fig. 7A**). As shown in **Fig. 7B**, a marked reduction in AHR was observed in mice administered with anti-CD109 mAb compared with those administered with isotype IgG (**Fig. 7B**). In addition, a decrease in total cell and eosinophil counts in BAL was also noted. Accordingly, bronchial wall thickening decreased with lower numbers of infiltrated inflammatory and $PAS^+$ cells in anti-CD109 mAb-administered mice (**Fig. 7D**). When anti-CD109 mAb were administered once on day 12, anti-CD109 mAb consistently suppressed AHR and eosinophilic airway inflammation (**Fig. S6**).

## DISCUSSION

The present study investigated a role of CD109 in development of AHR and eosinophilic airway inflammation. Interestingly, CD109 expression were inducible in lung cDC2s, but not



AJRCMB Articles in Press. Published October 10, 2022 as 10.1165/rcmb.2022-0109OC

in lung cDC1s, upon allergen challenges. Gene expression analyses showed that lung cDC2s from *CD109*$^{-/-}$ mice decreased eotaxin and Th2-related cytokines expression and increased some Th1 cytokines and *Runx3* expression. In addition, lung cDC2s from *CD109*$^{-/-}$ mice had poor capacity of antigen presentation and induction of cytokine production, such as IL-13, in *ex vivo* coculture with naïve T cells. Adoptive transfer of *CD109*$^{-/-}$ BMDCs failed to develop AHR with reduced eosinophilic inflammation. Finally, pharmacological modulation of CD109 by anti-CD109 mAb successfully reduced AHR and eosinophilic airway inflammation. Collectively, our results indicate a pivotal role of CD109 expressed on DCs in allergic airway inflammation, suggesting that CD109 regulation is a novel therapeutic target in asthma.

To the best of our knowledge, this study is the first to demonstrate the crucial role of CD109 in asthma pathogenesis. We showed that mice lacking the *CD109* gene develop markedly less AHR and eosinophilic airway inflammation with a significant decrease in Th2 cytokines (IL-4, IL-5, and IL-13) in the lung in asthma models. Peribronchial inflammation and PAS-positive cells were also significantly reduced. These observations suggest that mice lacking the *CD109* gene are resistant to asthmatic inflammation. CD109 was initially reported to negatively regulate TGF-β signaling. Indeed, mice overexpressing CD109 have less bleomycin-induced skin sclerosis than WT mice. (36) Recently, *CD109*$^{-/-}$ mice were also shown to be resistant to collagen-induced arthritis associated with decreased inflammatory cytokines. (19) Additionally, CD109 was shown to directly activate Janus kinase (Jak)-Stat3 signaling, which consequently leads to a metastatic phenotype in lung cancer cells. (13) Collectively, emerging evidence has demonstrated that CD109 is broadly involved in various pathological processes, such as inflammatory diseases. In this context, our data suggest that CD109 is required to develop the asthmatic phenotype in murine asthma



AJRCMB Articles in Press. Published October 10, 2022 as 10.1165/rcmb.2022-0109OC

models.

DCs play a critical role in orchestrating the adaptive immune response due to their unique ability to initiate a T cell response and direct differentiation into effector lineages. To initiate responses to highly disparate challenges, DCs have diversified into multiple phenotypically, anatomically, and functionally distinct cell types. (25, 28, 29) Our previous study showed that lung cDC2s, but not lung cDC1s, preferentially induced Th2 polarization. (31) This study showed that lung cDC2s from WT mice induced a large amount of IL-13, as well as IL-17A and IFN-γ in cocultures with naïve $CD4^+$ T cells from OT-II mice, although rational explanations could not be given for the elevated IL-2 concentration in the supernatant of *CD109*$^{-/-}$ lung cDC2s coculture. Interestingly, lung cDC2s from *CD109*$^{-/-}$ mice had reduced antigen uptake and T cell proliferation capacity, and increased cell death of cocultured OT-II $CD4^+$ T cells. This may be partly responsible for the reduced cytokine production in the supernatants of coculture of *CD109*$^{-/-}$ lung cDC2s and naïve OT-II $CD4^+$ T cells, compared to coculture of WT lung cDC2s and naïve OT-II $CD4^+$ T cells.

In addition, gene expression analysis showed that lung cDC2s from *CD109*$^{-/-}$ mice had decreased eotaxin (*Ccl24* and *Ccl26*) and Th2-related cytokine (*Il4*, *Il5*, *Il13*, and *Il33*) expression and increased expression of Th1-related cytokines (*Il18*, *Il12*, and *Cxcl9*), although the significances of DC-derived Th2 cytokines and eotaxin in allergic airway inflammation remains unclear. Th2 cells and ILC2, and epithelial cells, but not DCs, are found to be primarily involved in the production of Th2 cytokines and eotaxin, respectively. Impaired expression of *Ccl24*, *Ccl2, Cxcl9,* and increased expression of *Il12*in lung cDC2s from *CD109*$^{-/-}$ mice were possibly associated with less eosinophilic airway inflammation observed in allergen-challenged *CD109*$^{-/-}$ mice.

We further investigated CD109 expression in DCs in inducing AHR and eosinophilic airway inflammation in an asthma model using BMDCs. Intravenous injection



AJRCMB Articles in Press. Published October 10, 2022 as 10.1165/rcmb.2022-0109OC

of HDM-loaded WT BMDC and a subsequent intranasal HDM challenge or intratracheal challenge of WT BMDCs readily induced an increase of AHR, eosinophilic airway inflammation, and characteristic pathologic features of asthma. However, intravenous injection of HDM-loaded C*D109*$^{-/-}$ BMDCs and a subsequent intranasal HDM challenge exhibited no increase of AHR together with a significant smaller number of eosinophils and PAS-positive cells. In addition, intranasal challenge of HDM-loaded C*D109*$^{-/-}$ BMDCs also reduced allergic airway inflammation with decreased AHR. These observations suggest that CD109 expressed in DCs is required to elicit the asthmatic phenotype in this model during the sensitization and challenge phases.

Recently, novel cDC2 subsets, namely cDC2a and cDC2b were identified based on different expression patterns of transcription factors (26, 27). cDC2a are characterized by anti-inflammatory subsets with higher *RUNX3* and *T-bet* expression, while cDC2b has a pro-inflammatory phenotype with higher *RORγt* expression. Interestingly, lung cDC2s from *CD109*$^{-/-}$ mice had similar *RUNX3* and *RORγt* expression patterns to those of cDC2a. In addition, lung cDC2s from *CD109*$^{-/-}$ mice had poor ability to induce cytokines from naïve T cells and to proliferate naïve T cells. These characteristics of lung cDC2s from *CD109*$^{-/-}$ mice are similar to those of cDC2a. In particular, *RUNX3* was the most highly expressed transcriptional factor in lung cDC2s from *CD109*$^{-/-}$ mice. RUNX3, of the Runt-related transcription factor family, plays an important role in developing immune systems, especially T cell differentiation. (37-40) RUNX3 functions as a component of the TGF-β signaling cascade of the SMAD pathway. RUNX3 corporately binds to the *Ifg* promoter and *Il4* silencer, resulting in Th2 cytokine production repression. (37) Importantly, several lines of studies suggest the involvement of RUNX3 in asthma pathogenesis; decreased RUNX3 levels in the lungs of experimental asthma, (41) and reduced RUNX3 expression in CD4$^{+}$ T cells in



AJRCMB Articles in Press. Published October 10, 2022 as 10.1165/rcmb.2022-0109OC

patients with asthma. (42, 43) Furthermore, *RUNX3* in PBMC were hypomethylated in patients with asthma as similar to those of *IL4* and *IL13*. (44) RUNX3 has been also shown to govern DC function. BMDCs from *RUNX3*$^{-/-}$ mice showed a hyperactivated state, and *RUNX3*$^{-/-}$mice spontaneously develop asthma-like airway inflammation with the accumulation of hyperactivated DCs. (45) Interestingly, RUNX3 in cDC2s was reported responsible for maintaining intestinal immune tolerance through its immune regulatory functions. (46) Collectively these findings suggest that RUNX3 in DCs, particularly cDC2s, suppresses a Th2-mediated immune response. In accordance with these, we found that lung cDC2s from *CD109*$^{-/-}$ mice had a significantly increased RUNX3 expression compared to WT mice. This expression may be partly associated with ameliorating the asthmatic phenotype observed in *CD109*$^{-/-}$ mice.

Finally, we showed that the administration of anti-CD109 mAb during either allergen sensitization or allergen challenge completely abolished increased AHR and significantly decreased eosinophil recruitment in murine asthma models. In addition, anti-CD109 mAb also reduced peribronchiolar inflammation and PAS-positive cells. These observations indicate that anti-CD109 mAb successfully improves the asthmatic phenotype of the murine models of asthma. Several mAbs that target IL-5, IL-13, IL-33, IgE, and thymic stromal lymphopoietin (TSLP) are clinically available. (47) However, the efficacy of established biologic therapies are heterogenous in terms of exacerbation, airflow limitation, glucocorticoid-sparing effects, and asthma phenotypes (Th2-high, Th2-low, FeNO-high, FeNO-low, blood eosinophil counts-high and blood eosinophil counts-low); the development of more broadly effective biologics is desired. In this regard, this study suggests that mAb against CD109 may be a novel therapeutic option for asthma. Further research is required to



AJRCMB Articles in Press. Published October 10, 2022 as 10.1165/rcmb.2022-0109OC

clarify this possibility.

In conclusion, this study showed that mice lacking *CD109* gene suppressed the development of AHR and eosinophilic inflammation in the murine models of asthma. Deficit expression of CD109 in lung cDC2s may be critical in this suppression. Moreover, administration of anti-CD109 mAb during either allergen sensitization or allergen challenge phases successfully attenuated asthmatic phenotypes, such as increased AHR and eosinophilic airway inflammation. Taken together, the present study provides new insights into the involvement of CD109 in pathogenesis of asthma, suggesting that CD109 is a novel therapeutic target for asthma.



AJRCMB Articles in Press. Published October 10, 2022 as 10.1165/rcmb.2022-0109OC

**Figure legends**

**Figure 1.** Lack of CD109 ameliorated airway hyperreactivity and eosinophilic airway inflammation.

(**A**) Experimental timeline. WT and CD109$^{-/-}$ mice were intranasally (i.n.) sensitized and challenged with house dust mite (HDM). (B) Lung resistance ($R_L$) and dynamic compliance ($C_{dyn}$), (n = 5–7 per group). (**C**) Differential cell counts in BAL (n = 5–7 per group). TCC, total cell count; Eos, eosinophils. (**D**). Hematoxylin and eosin and PAS staining. Original magnification: 100×, scale bar: 50 μm. Quantifications of lung histopathology (n = 6 per group). (**E**) Cytokine levels in lung homogenates (n = 6 per group). Data are representative of at least five independent experiments. (**F**) Total IgE, HDM-specific IgE and IgG1 levels in serum (n = 5–6 per group). Data are representative of at least two independent experiments and shown as the mean ± SEM. P-values were calculated using Student's *t*-test and one-way ANOVA post hoc test with Tukey's multiple comparison test. *P < 0.05, **P < 0.01, ***P < 0.001.

**Figure 2**. CD109 expression was inducible after allergen sensitization.

(**A**) WT mice were sensitized with OVA + Alum on days 1 and 8 and challenged with OVA for three consecutive days (days 18 to 20) as described in **Fig S1A**. Subsequently, CD109 expression in lung immune cells was analyzed on day 21. Representative FACS histogram and mean fluorescence intensity (MFI) of CD109 (n = 3–4 per group). (**B**) WT mice were immunized as described in **Fig 1A,** and cell-surface markers in CD109$^+$ lung DCs and CD109$^-$ lung DCs were analyzed. Gating strategy of CD109$^+$ lung DCs and CD109$^-$ lung DCs. (**C**) Representative FACS histogram and mean fluorescence intensity (n = 6 per group).



AJRCMB Articles in Press. Published October 10, 2022 as 10.1165/rcmb.2022-0109OC

Data are representative of two independent experiments. *P < 0.05, ***P < 0.001.

**Figure 3.** Lung cDC2s from *CD109*$^{-/-}$ mice had poor capacity of antigen presentation, and showed impaired cytokine production in ex vivo coculture with naïve T cells.

Sorted lung dendritic cell (DC) subsets were cocultured with naïve CD4$^{+}$ T cells isolated from OT-II mice in the presence of $OVA_{323–339}$ peptide for seven days. (**A**) Experimental timeline. WT and *CD109*$^{-/-}$ mice were intraperitoneally immunized with OVA and alum adjuvant and intranasally challenged with OVA. Subsequently, lung DC subsets were isolated. (**B**) Identification of lung DC subsets; cDC1 and cDC2. Representative FACS plots. (**C**) Cytokine levels in cDC2-CD4$^{+}$T cell coculture supernatants (n = 9 per group). (**D**) Proliferation of cocultured CD4$^{+}$ T cells measured on day3 by CellTrace Violet staining (n = 4 per group). Representative FACS histogram and percentage of divided cells. (**E**) Annexin V and propidium iodide staining were performed on cocultured CD4$^{+}$ T cells on day 7 (n = 3 per group). Representative FACS plots and percentage of apoptotic cells (Annexin V$^{+}$ cells). (**F**) Mice were immunized and challenged as described in **Fig. 3A.** In the last challenge (day20), fluoresceine-labeled OVA was intranasally administered to assess capability of antigen presentation of DCs. FACS histogram and MFI of fluoresceine-labeled OVA in each cDC2s were assessed (n = 5 per group).

Data are representative of two experiments and shown as the mean ± SEM. P-values were calculated using Student's *t*-test. *P < 0.05, ***P < 0.001.

**Figure 4.** CD109 expression in DCs was responsible for the induction of asthmatic phenotype.



AJRCMB Articles in Press. Published October 10, 2022 as 10.1165/rcmb.2022-0109OC

(**A**) Experimental timeline. Cultured BMDCs from WT or *CD109*$^{-/-}$ mice were stimulated with house dust mite (HDM) for six hours and then intravenously injected into WT mice. Then mice were intratracheally challenged with HDM on day1, and challenged with HDM on days 8 and 13. (**B**) Lung resistance ($R_L$) and dynamic compliance ($C_{dyn}$), (n = 6–7 per group). (**C**) Differential cell counts in BAL (n = 7 per group). TCC, total cell count; Eos, eosinophils. (**D**). Hematoxylin and eosin and PAS staining. Original magnification: 100×, scale bar: 50 μm. Quantifications of lung histopathology (n = 7 per group). Data are representative of two independent experiments and expressed as mean ± SEM. P-values were calculated using Student's *t*-test and one-way ANOVA post hoc test with Tukey's multiple comparison test. *P < 0.05, **P < 0.01.

**Figure 5.** Gene expression analyzes in *CD109*$^{-/-}$ lung DC subsets.

WT and *CD109*$^{-/-}$ mice were immunized as described in **Fig 1A,** and lung cDC2s were isolated as described in **Fig 3B**. (**A**) Heat plots showing alternations of depicted genes in lung cDC2s in WT and *CD109*$^{-/-}$ mice (n = 3). (**B**) Representative FACS histogram and mean fluorescence intensity (MFI) of RUNX3 in lung cDC2s (n = 3). (**C**) Representative FACS histogram and mean fluorescence intensity (MFI) of SMAD2/3 phosphorylation in lung cDC2s (n = 5). Data were representative of two independent experiments and expressed as mean ± SEM. P-values were calculated using Student's *t*-test. *P < 0.05 *, **P < 0.01.

**Figure 6.** Anti-CD109 monoclonal antibody ameliorated AHR and eosinophilic airway inflammation during allergen sensitization.



AJRCMB Articles in Press. Published October 10, 2022 as 10.1165/rcmb.2022-0109OC

(**A**) Experimental timeline. WT mice were immunized as described in **Fig 1A**. Anti-CD109 monoclonal antibody or isotype IgG were intranasally administered before the house dust mite (HDM) sensitization (day0). (**B**) Lung resistance ($R_L$) and dynamic compliance ($C_{dyn}$), (n = 6–7 per group). (**C**) Differential cell counts in BAL (n = 6–7 per group). TCC, total cell count; Eos, eosinophils. (**D**). Hematoxylin and eosin and PAS staining. Original magnification: 100×, scale bar: 50 μm. Quantification of lung histopathology (n = 6 per group). Data are representative of two independent experiments. Data are representative of two independent experiments and expressed as mean ± SEM. P-values were calculated using Student's *t*-test and one-way ANOVA post hoc test with Tukey's multiple comparison test. *P < 0.05, **P < 0.01, ***P < 0.001.

**Figure 7.** Anti-CD109 monoclonal antibody ameliorated AHR and eosinophilic airway inflammation during allergen sensitization and allergen challenge.

(**A**) Experimental timeline. WT mice were immunized as described in **Fig 1A**. Anti-CD109 monoclonal antibody or isotype IgG were intranasally administered on day7,12 before the house dust mite (HDM) challenge. (**B**) Lung resistance ($R_L$) and dynamic compliance ($C_{dyn}$), (n = 6–7 per group). (**C**) Differential cell counts in BAL (n = 6–7 per group). TCC, total cell count; Eos, eosinophils. (**D**). Hematoxylin and eosin and PAS staining. Original magnification: 100×, scale bar: 50 μm. Quantification of lung histopathology (n = 6 per group). Data are representative of two independent experiments and expressed as mean ± SEM. P-values were calculated using Student's *t*-test and one-way ANOVA post hoc test



AJRCMB Articles in Press. Published October 10, 2022 as 10.1165/rcmb.2022-0109OC

with Tukey's multiple comparison test. *P < 0.05, **P < 0.01, ***P < 0.001.



AJRCMB Articles in Press. Published October 10, 2022 as 10.1165/rcmb.2022-0109OC

## REFERENCES

1. Lambrecht BN, Hammad H. The role of dendritic and epithelial cells as master regulators of allergic airway inflammation. *Lancet (London, England)* 2010; 376: 835-843.

2. Brusselle G, Bracke K. Targeting immune pathways for therapy in asthma and chronic obstructive pulmonary disease. *Annals of the American Thoracic Society* 2014; 11 Suppl 5: S322-328.

3. Brusselle GG, Maes T, Bracke KR. Eosinophils in the spotlight: Eosinophilic airway inflammation in nonallergic asthma. *Nat Med* 2013; 19: 977-979.

4. Wenzel SE. Asthma phenotypes: the evolution from clinical to molecular approaches. *Nat Med* 2012; 18: 716-725.

5. Halim TY, Steer CA, Matha L, Gold MJ, Martinez-Gonzalez I, McNagny KM, McKenzie AN, Takei F. Group 2 innate lymphoid cells are critical for the initiation of adaptive T helper 2 cell-mediated allergic lung inflammation. *Immunity* 2014; 40: 425-435.

6. Maazi H, Banie H, Aleman Muench GR, Patel N, Wang B, Sankaranarayanan I, Bhargava V, Sato T, Lewis G, Cesaroni M, Karras J, Das A, Soroosh P, Akbari O. Activated plasmacytoid dendritic cells regulate type 2 innate lymphoid cell-mediated airway hyperreactivity. *The Journal of allergy and clinical immunology* 2018; 141: 893-905 e896.

7. Lin M, Sutherland DR, Horsfall W, Totty N, Yeo E, Nayar R, Wu XF, Schuh AC. Cell surface antigen CD109 is a novel member of the alpha(2) macroglobulin/C3, C4, C5 family of thioester-containing proteins. *Blood* 2002; 99: 1683-1691.

8. Mii S, Enomoto A, Shiraki Y, Taki T, Murakumo Y, Takahashi M. CD109: a multifunctional GPI-anchored protein with key roles in tumor progression and physiological homeostasis. *Pathol Int* 2019; 69: 249-259.

9. Bizet AA, Liu K, Tran-Khanh N, Saksena A, Vorstenbosch J, Finnson KW, Buschmann



AJRCMB Articles in Press. Published October 10, 2022 as 10.1165/rcmb.2022-0109OC

MD, Philip A. The TGF-β co-receptor, CD109, promotes internalization and degradation of TGF-β receptors. *Biochim Biophys Acta* 2011; 1813: 742-753.

10. Li C, Hancock MA, Sehgal P, Zhou S, Reinhardt DP, Philip A. Soluble CD109 binds TGF-β and antagonizes TGF-β signalling and responses. *Biochem J* 2016; 473: 537-547.

11. Vorstenbosch J, Nguyen CM, Zhou S, Seo YJ, Siblini A, Finnson KW, Bizet AA, Tran SD, Philip A. Overexpression of CD109 in the Epidermis Differentially Regulates ALK1 Versus ALK5 Signaling and Modulates Extracellular Matrix Synthesis in the Skin. *J Invest Dermatol* 2017; 137: 641-649.

12. Tsai YL, Ha DP, Zhao H, Carlos AJ, Wei S, Pun TK, Wu K, Zandi E, Kelly K, Lee AS. Endoplasmic reticulum stress activates SRC, relocating chaperones to the cell surface where GRP78/CD109 blocks TGF-β signaling. *Proceedings of the National Academy of Sciences of the United States of America* 2018; 115: E4245-e4254.

13. Chuang CH, Greenside PG, Rogers ZN, Brady JJ, Yang D, Ma RK, Caswell DR, Chiou SH, Winters AF, Gruner BM, Ramaswami G, Spencley AL, Kopecky KE, Sayles LC, Sweet-Cordero EA, Li JB, Kundaje A, Winslow MM. Molecular definition of a metastatic lung cancer state reveals a targetable CD109-Janus kinase-Stat axis. *Nat Med* 2017; 23: 291-300.

14. Hagikura M, Murakumo Y, Hasegawa M, Jijiwa M, Hagiwara S, Mii S, Hagikura S, Matsukawa Y, Yoshino Y, Hattori R, Wakai K, Nakamura S, Gotoh M, Takahashi M. Correlation of pathological grade and tumor stage of urothelial carcinomas with CD109 expression. *Pathol Int* 2010; 60: 735-743.

15. Hagiwara S, Murakumo Y, Mii S, Shigetomi T, Yamamoto N, Furue H, Ueda M, Takahashi M. Processing of CD109 by furin and its role in the regulation of TGF-beta signaling. *Oncogene* 2010; 29: 2181-2191.



AJRCMB Articles in Press. Published October 10, 2022 as 10.1165/rcmb.2022-0109OC

16. Hashimoto M, Ichihara M, Watanabe T, Kawai K, Koshikawa K, Yuasa N, Takahashi T, Yatabe Y, Murakumo Y, Zhang JM, Nimura Y, Takahashi M. Expression of CD109 in human cancer. *Oncogene* 2004; 23: 3716-3720.

17. Dai J, Li ZX, Zhang Y, Ma JL, Zhou T, You WC, Li WQ, Pan KF. Whole Genome Messenger RNA Profiling Identifies a Novel Signature to Predict Gastric Cancer Survival. *Clin Transl Gastroenterol* 2019; 10: e00004.

18. Shiraki Y, Mii S, Enomoto A, Momota H, Han YP, Kato T, Ushida K, Kato A, Asai N, Murakumo Y, Aoki K, Suzuki H, Ohka F, Wakabayashi T, Todo T, Ogawa S, Natsume A, Takahashi M. Significance of perivascular tumour cells defined by CD109 expression in progression of glioma. *J Pathol* 2017; 243: 468-480.

19. Song G, Feng T, Zhao R, Lu Q, Diao Y, Guo Q, Wang Z, Zhang Y, Ge L, Pan J, Wang L, Han J. CD109 regulates the inflammatory response and is required for the pathogenesis of rheumatoid arthritis. *Ann Rheum Dis* 2019; 78: 1632-1641.

20. Zhang H, Carnevale G, Polese B, Simard M, Thurairajah B, Khan N, Gentile ME, Fontes G, Vinh DC, Pouliot R, King IL. CD109 Restrains Activation of Cutaneous IL-17-Producing gammadelta T Cells by Commensal Microbiota. *Cell Rep* 2019; 29: 391-405 e395.

21. Mii S, Murakumo Y, Asai N, Jijiwa M, Hagiwara S, Kato T, Asai M, Enomoto A, Ushida K, Sobue S, Ichihara M, Takahashi M. Epidermal hyperplasia and appendage abnormalities in mice lacking CD109. *Am J Pathol* 2012; 181: 1180-1189.

22. Galle-Treger L, Suzuki Y, Patel N, Sankaranarayanan I, Aron JL, Maazi H, Chen L, Akbari O. Nicotinic acetylcholine receptor agonist attenuates ILC2-dependent airway hyperreactivity. *Nature communications* 2016; 7: 13202.

23. Suzuki Y, Maazi H, Sankaranarayanan I, Lam J, Khoo B, Soroosh P, Barbers RG, James Ou JH, Jung JU, Akbari O. Lack of autophagy induces steroid-resistant airway



AJRCMB Articles in Press. Published October 10, 2022 as 10.1165/rcmb.2022-0109OC

inflammation. *The Journal of allergy and clinical immunology* 2016; 137: 1382-1389.e1389.

24. Suzuki Y, Aono Y, Akiyama N, Horiike Y, Naoi H, Horiguchi R, Shibata K, Hozumi H, Karayama M, Furuhashi K, Enomoto N, Fujisawa T, Nakamura Y, Inui N, Suda T. Involvement of autophagy in exacerbation of eosinophilic airway inflammation in a murine model of obese asthma. *Autophagy*.
25. Guilliams M, Ginhoux F, Jakubzick C, Naik SH, Onai N, Schraml BU, Segura E, Tussiwand R, Yona S. Dendritic cells, monocytes and macrophages: a unified nomenclature based on ontogeny. *Nature Reviews Immunology* 2014; 14: 571-578.
26. Brown CC, Gudjonson H, Pritykin Y, Deep D, Lavallee VP, Mendoza A, Fromme R, Mazutis L, Ariyan C, Leslie C, Pe'er D, Rudensky AY. Transcriptional Basis of Mouse and Human Dendritic Cell Heterogeneity. *Cell* 2019; 179: 846-863 e824.
27. Nutt SL, Chopin M. Transcriptional Networks Driving Dendritic Cell Differentiation and Function. *Immunity* 2020; 52: 942-956.
28. Sakurai S, Furuhashi K, Horiguchi R, Nihashi F, Yasui H, Karayama M, Suzuki Y, Hozumi H, Enomoto N, Fujisawa T, Nakamura Y, Inui N, Suda T. Conventional type 2 lung dendritic cells are potent inducers of follicular helper T cells in the asthmatic lung. *Allergology international : official journal of the Japanese Society of Allergology* 2021; 70: 351-359.
29. Murphy TL, Grajales-Reyes GE, Wu X, Tussiwand R, Briseño CG, Iwata A, Kretzer NM, Durai V, Murphy KM. Transcriptional Control of Dendritic Cell Development. *Annual review of immunology* 2016; 34: 93-119.
30. Suzuki Y, Suda T, Furuhashi K, Shibata K, Hashimoto D, Enomto N, Fujisawa T, Nakamura Y, Inui N, Nakamura H, Chida K. Mouse CD11bhigh lung dendritic cells have more potent capability to induce IgA than CD103+ lung dendritic cells in vitro.



AJRCMB Articles in Press. Published October 10, 2022 as 10.1165/rcmb.2022-0109OC

*American journal of respiratory cell and molecular biology* 2012; 46: 773-780.

31. Furuhashi K, Suda T, Hasegawa H, Suzuki Y, Hashimoto D, Enomoto N, Fujisawa T, Nakamura Y, Inui N, Shibata K, Nakamura H, Chida K. Mouse lung CD103+ and CD11bhigh dendritic cells preferentially induce distinct CD4+ T-cell responses. *American journal of respiratory cell and molecular biology* 2012; 46: 165-172.
32. Gao Y, Nish Simone A, Jiang R, Hou L, Licona-Limón P, Weinstein Jason S, Zhao H, Medzhitov R. Control of T Helper 2 Responses by Transcription Factor IRF4-Dependent Dendritic Cells. *Immunity* 2013; 39: 722-732.
33. Kumamoto Y, Linehan M, Weinstein Jason S, Laidlaw Brian J, Craft Joseph E, Iwasaki A. CD301b+ Dermal Dendritic Cells Drive T Helper 2 Cell-Mediated Immunity. *Immunity* 2013; 39: 733-743.
34. Williams JW, Tjota MY, Clay BS, Vander Lugt B, Bandukwala HS, Hrusch CL, Decker DC, Blaine KM, Fixsen BR, Singh H, Sciammas R, Sperling AI. Transcription factor IRF4 drives dendritic cells to promote Th2 differentiation. *Nature communications* 2013; 4.
35. van Rijt LS, Jung S, Kleinjan A, Vos N, Willart M, Duez C, Hoogsteden HC, Lambrecht BN. In vivo depletion of lung CD11c+ dendritic cells during allergen challenge abrogates the characteristic features of asthma. *J Exp Med* 2005; 201: 981-991.
36. Vorstenbosch J, Al-Ajmi H, Winocour S, Trzeciak A, Lessard L, Philip A. CD109 overexpression ameliorates skin fibrosis in a mouse model of bleomycin-induced scleroderma. *Arthritis Rheum* 2013; 65: 1378-1383.
37. Djuretic IM, Levanon D, Negreanu V, Groner Y, Rao A, Ansel KM. Transcription factors T-bet and Runx3 cooperate to activate Ifng and silence Il4 in T helper type 1 cells. *Nat Immunol* 2007; 8: 145-153.
38. Ebihara T, Song C, Ryu SH, Plougastel-Douglas B, Yang L, Levanon D, Groner Y, Bern



AJRCMB Articles in Press. Published October 10, 2022 as 10.1165/rcmb.2022-0109OC

MD, Stappenbeck TS, Colonna M, Egawa T, Yokoyama WM. Runx3 specifies lineage commitment of innate lymphoid cells. *Nat Immunol* 2015; 16: 1124-1133.

39. Yu Y, Wang L, Gu G. The correlation between Runx3 and bronchial asthma. *Clin Chim Acta* 2018; 487: 75-79.

40. Shan Q, Zeng Z, Xing S, Li F, Hartwig SM, Gullicksrud JA, Kurup SP, Van Braeckel-Budimir N, Su Y, Martin MD, Varga SM, Taniuchi I, Harty JT, Peng W, Badovinac VP, Xue HH. The transcription factor Runx3 guards cytotoxic CD8(+) effector T cells against deviation towards follicular helper T cell lineage. *Nat Immunol* 2017; 18: 931-939.

41. Zhou X, Zhu J, Bian T, Wang R, Gao F. Mislocalization of Runt-related transcription factor 3 results in airway inflammation and airway hyper-responsiveness in a murine asthma model. *Exp Ther Med* 2017; 14: 2695-2701.

42. Fan L, Wang X, Fan L, Chen Q, Zhang H, Pan H, Xu A, Wang H, Yu Y. MicroRNA-145 influences the balance of Th1/Th2 via regulating RUNX3 in asthma patients. *Experimental lung research* 2016; 42: 417-424.

43. Qiu YY, Zhang YW, Qian XF, Bian T. miR-371, miR-138, miR-544, miR-145, and miR-214 could modulate Th1/Th2 balance in asthma through the combinatorial regulation of Runx3. *Am J Transl Res* 2017; 9: 3184-3199.

44. Yang IV, Pedersen BS, Liu A, O'Connor GT, Teach SJ, Kattan M, Misiak RT, Gruchalla R, Steinbach SF, Szefler SJ, Gill MA, Calatroni A, David G, Hennessy CE, Davidson EJ, Zhang W, Gergen P, Togias A, Busse WW, Schwartz DA. DNA methylation and childhood asthma in the inner city. *The Journal of allergy and clinical immunology* 2015; 136: 69-80.

45. Fainaru O, Woolf E, Lotem J, Yarmus M, Brenner O, Goldenberg D, Negreanu V, Bernstein Y, Levanon D, Jung S, Groner Y. Runx3 regulates mouse TGF-beta-



AJRCMB Articles in Press. Published October 10, 2022 as 10.1165/rcmb.2022-0109OC

mediated dendritic cell function and its absence results in airway inflammation. *Embo j* 2004; 23: 969-979.

46. Hantisteanu S, Dicken Y, Negreanu V, Goldenberg D, Brenner O, Leshkowitz D, Lotem J, Levanon D, Groner Y. Runx3 prevents spontaneous colitis by directing the differentiation of anti-inflammatory mononuclear phagocytes. *PLoS One* 2020; 15: e0233044.

47. Wechsler ME, Ruddy MK, Pavord ID, Israel E, Rabe KF, Ford LB, Maspero JF, Abdulai RM, Hu CC, Martincova R, Jessel A, Nivens MC, Amin N, Weinreich DM, Yancopoulos GD, Goulaouic H. Efficacy and Safety of Itepekimab in Patients with Moderate-to-Severe Asthma. *N Engl J Med* 2021; 385: 1656-1668.



AJRCMB Articles in Press. Published October 10, 2022 as 10.1165/rcmb.2022-0109OC

**Figure 1.** Lack of CD109 ameliorated airway hyperreactivity and eosinophilic airway inflammation.

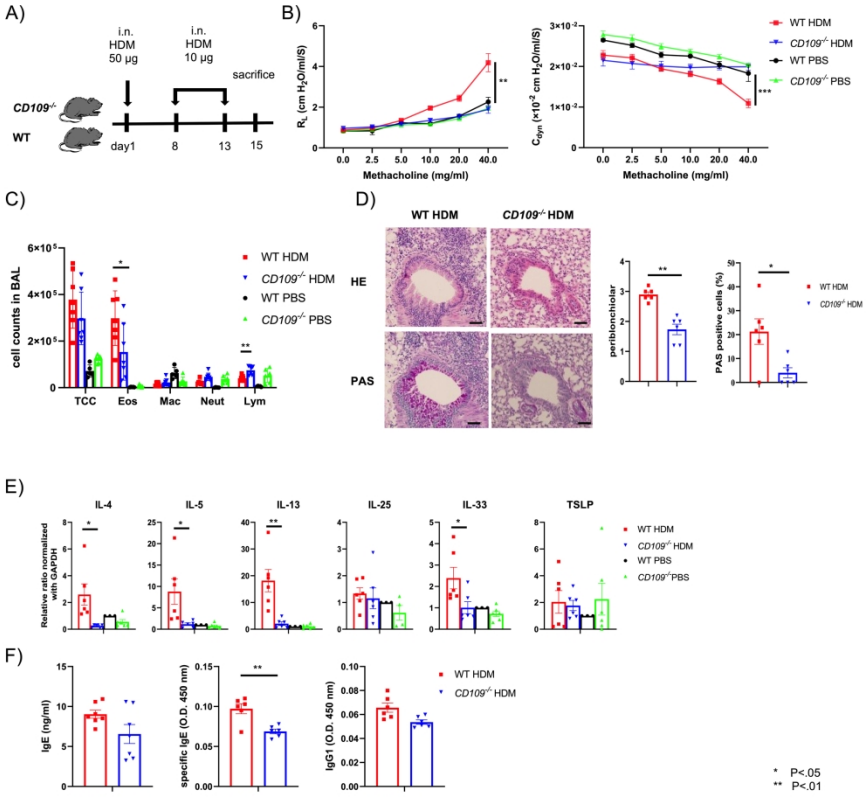


Figure 1. Lack of CD109 ameliorated airway hyperreactivity and eosinophilic airway inflammation. (A) Experimental timeline. WT and CD109−/− mice were intranasally (i.n.) sensitized and challenged with house dust mite (HDM). (B) Lung resistance (RL) and dynamic compliance (Cdyn), (n = 5–7 per group). (C) Differential cell counts in BAL (n = 5–7 per group). TCC, total cell count; Eos, eosinophils. (D). Hematoxylin and eosin and PAS staining. Original magnification: 100☐, scale bar: 50 µm. Quantifications of lung histopathology (n = 6 per group). (E) Cytokine levels in lung homogenates (n = 6 per group). Data are representative of at least five independent experiments. (F) Total IgE, HDM-specific IgE and IgG1 levels in serum (n = 5–6 per group). Data are representative of at least two independent experiments and shown as the mean ± SEM. P-values were calculated using Student's t-test and one-way ANOVA post hoc test with Tukey's multiple comparison test. *P < 0.05, **P < 0.01, ***P < 0.001.

249x211mm (300 x 300 DPI)

AJRCMB Articles in Press. Published October 10, 2022 as 10.1165/rcmb.2022-0109OC

**Figure 2.** CD109 expression was inducible after allergen sensitization.

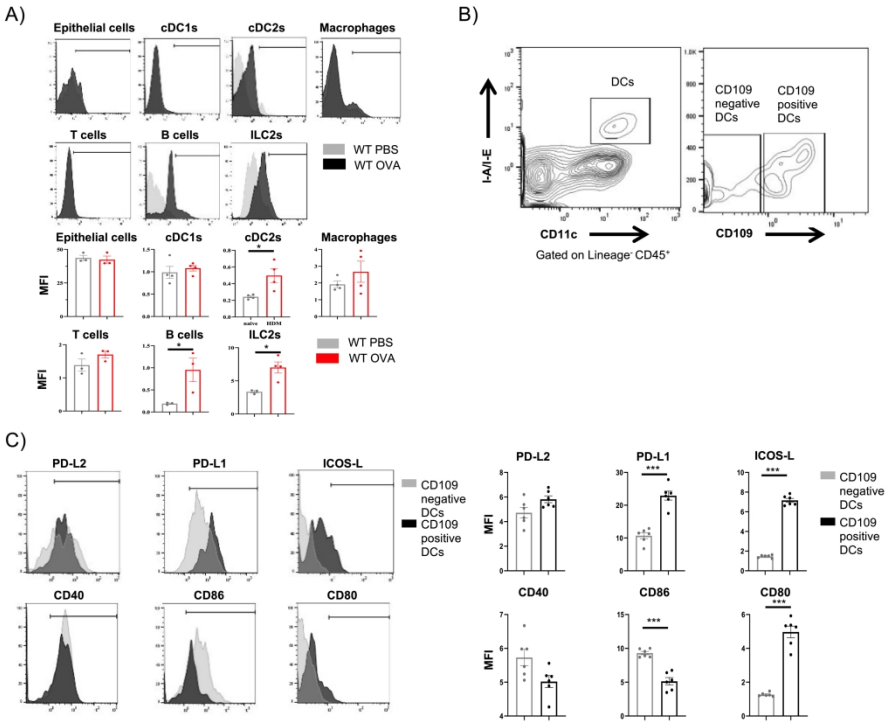


Figure 2. CD109 expression was inducible after allergen sensitization.
(A) WT mice were sensitized with OVA + Alum on days 1 and 8 and challenged with OVA for three consecutive days (days 18 to 20) as described in Fig S1A. Subsequently, CD109 expression in lung immune cells was analyzed on day 21. Representative FACS histogram and mean fluorescence intensity (MFI) of CD109 (n = 3–4 per group). (B) WT mice were immunized as described in Fig 1A, and cell-surface markers in CD109+ lung DCs and CD109− lung DCs were analyzed. Gating strategy of CD109+ lung DCs and CD109− lung DCs. (C) Representative FACS histogram and mean fluorescence intensity (n = 6 per group). Data are representative of two independent experiments. *P < 0.05, ***P < 0.001.

270x209mm (300 x 300 DPI)

AJRCMB Articles in Press. Published October 10, 2022 as 10.1165/rcmb.2022-0109OC

**Figure 3.** Lung cDC2s from CD109$^{-/-}$ mice had poor capability of antigen presentation, and showed impaired cytokine production in ex vivo cocultures with naïve T cells.

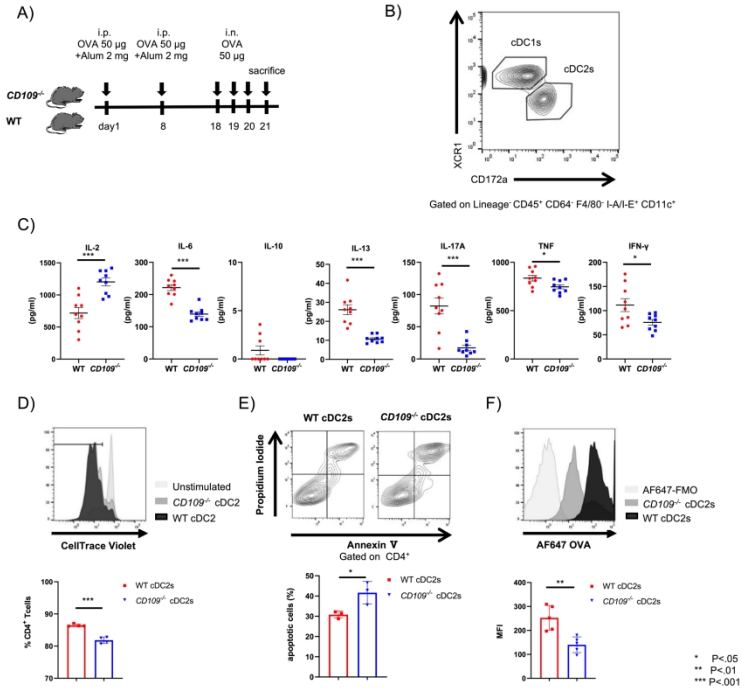


Figure 3. Lung cDC2s from CD109−/− mice had poor capacity of antigen presentation, and showed impaired cytokine production in ex vivo coculture with naïve T cells.
Sorted lung dendritic cell (DC) subsets were cocultured with naïve CD4+ T cells isolated from OT-II mice in the presence of OVA323–339 peptide for seven days. (A) Experimental timeline. WT and CD109−/− mice were intraperitoneally immunized with OVA and alum adjuvant and intranasally challenged with OVA. Subsequently, lung DC subsets were isolated. (B) Identification of lung DC subsets; cDC1 and cDC2. Representative FACS plots. (C) Cytokine levels in cDC2-CD4+T cell coculture supernatants (n = 9 per group). (D) Proliferation of cocultured CD4+ T cells measured on day3 by CellTrace Violet staining (n = 4 per group). Representative FACS histogram and percentage of divided cells. (E) Annexin V and propidium iodide staining were performed on cocultured CD4+ T cells on day 7 (n = 3 per group). Representative FACS plots and percentage of apoptotic cells (Annexin V+ cells). (F) Mice were immunized and challenged as described in Fig. 3A. In the last challenge (day20), fluoresceine-labeled OVA was intranasally administered to assess capability of antigen presentation of DCs. FACS histogram and MFI of fluoresceine-labeled OVA in each cDC2s were assessed (n = 5 per group).
Data are representative of two experiments and shown as the mean ± SEM. P-values were calculated using Student's t-test. *P < 0.05, ***P < 0.001.

280x210mm (300 x 300 DPI)

AJRCMB Articles in Press. Published October 10, 2022 as 10.1165/rcmb.2022-0109OC

**Figure 4.** CD109 expression in DCs was responsible for the induction of asthmatic phenotype.

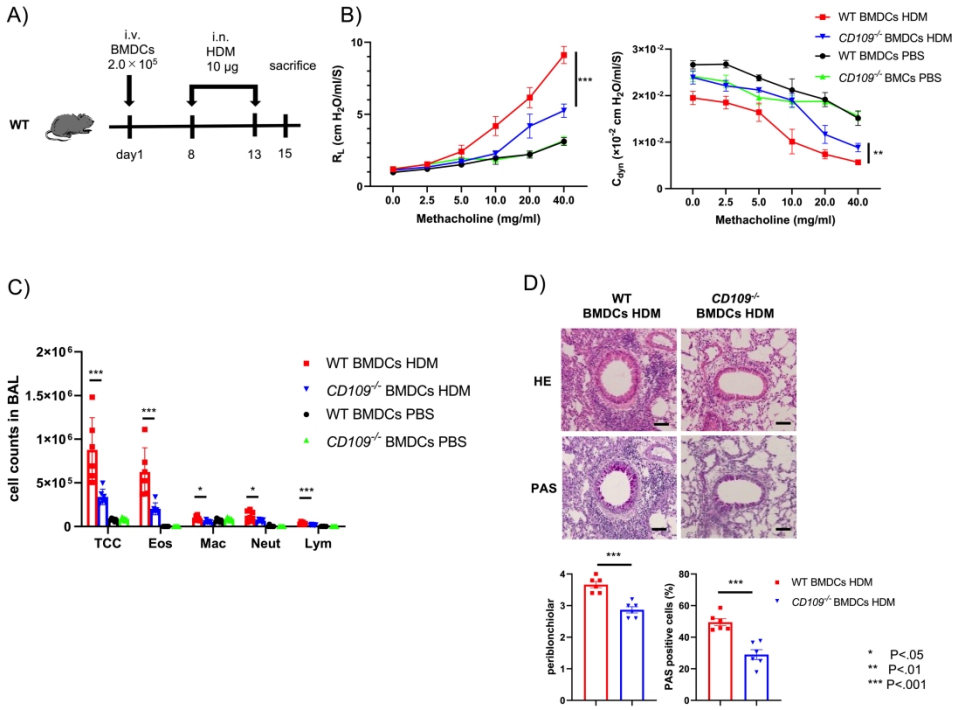


Figure 4. CD109 expression in DCs was responsible for the induction of asthmatic phenotype. (A) Experimental timeline. Cultured BMDCs from WT or CD109−/− mice were stimulated with house dust mite (HDM) for six hours and then intravenously injected into WT mice. Then mice were intratracheally challenged with HDM on day1, and challenged with HDM on days 8 and 13. (B) Lung resistance (RL) and dynamic compliance (Cdyn), (n = 6–7 per group). (C) Differential cell counts in BAL (n = 7 per group). TCC, total cell count; Eos, eosinophils. (D). Hematoxylin and eosin and PAS staining. Original magnification: 100□, scale bar: 50 μm. Quantifications of lung histopathology (n = 7 per group). Data are representative of two independent experiments and expressed as mean ± SEM. P-values were calculated using Student's t-test and one-way ANOVA post hoc test with Tukey's multiple comparison test. *P < 0.05, **P < 0.01.

281x211mm (300 x 300 DPI)

AJRCMB Articles in Press. Published October 10, 2022 as 10.1165/rcmb.2022-0109OC

**Figure 5.** Gene expression analyzes in *CD109*$^{-/-}$ lung DC subsets.

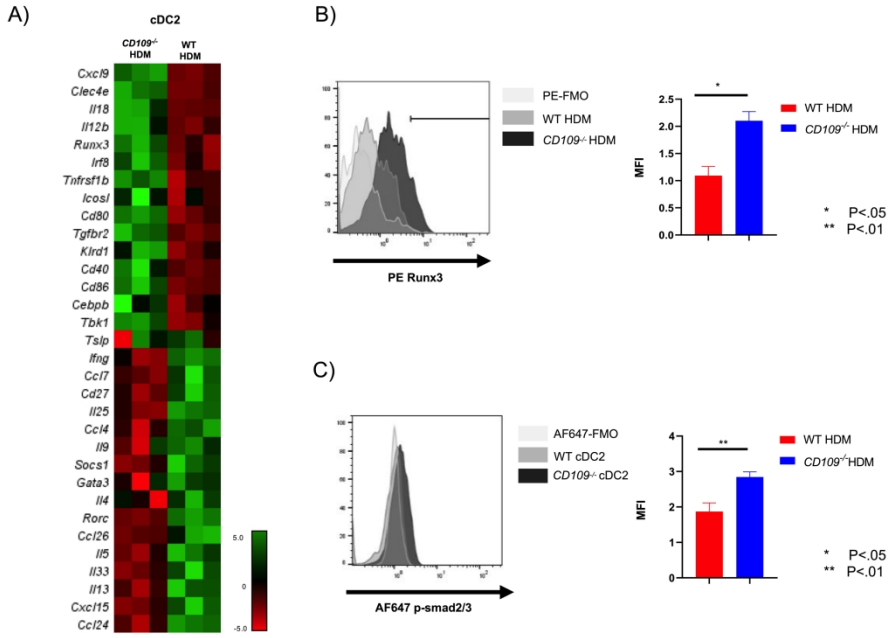


Figure 5. Gene expression analyzes in CD109−/− lung DC subsets.
WT and CD109−/− mice were immunized as described in Fig 1A, and lung cDC2s were isolated as described in Fig 3B. (A) Heat plots showing alternations of depicted genes in lung cDC2s in WT and CD109−/− mice (n = 3). (B) Representative FACS histogram and mean fluorescence intensity (MFI) of RUNX3 in lung cDC2s (n = 3). (C) Representative FACS histogram and mean fluorescence intensity (MFI) of SMAD2/3 phosphorylation in lung cDC2s (n = 5). Data were representative of two independent experiments and expressed as mean ± SEM. P-values were calculated using Student's t-test. *P < 0.05 *, **P < 0.01.

270x211mm (300 x 300 DPI)

AJRCMB Articles in Press. Published October 10, 2022 as 10.1165/rcmb.2022-0109OC

**Figure 6.** Anti-CD109 monoclonal antibody ameliorated AHR and eosinophilic airway inflammation during allergen sensitization.

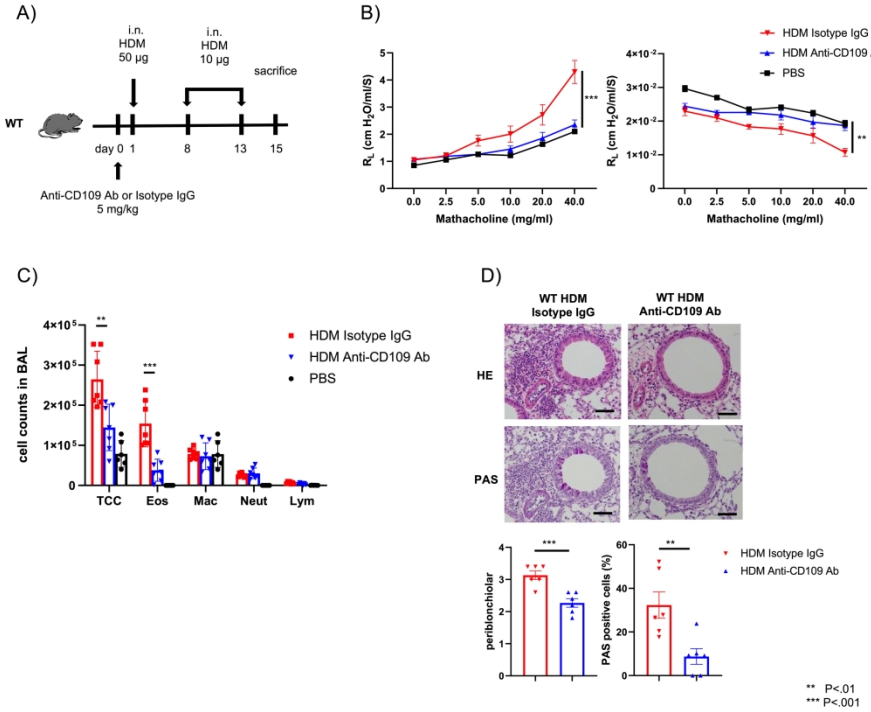


Figure 6. Anti-CD109 monoclonal antibody ameliorated AHR and eosinophilic airway inflammation during allergen sensitization.

(A) Experimental timeline. WT mice were immunized as described in Fig 1A. Anti-CD109 monoclonal antibody or isotype IgG were intranasally administered before the house dust mite (HDM) sensitization (day0). (B) Lung resistance (RL) and dynamic compliance (Cdyn), (n = 6–7 per group). (C) Differential cell counts in BAL (n = 6–7 per group). TCC, total cell count; Eos, eosinophils. (D). Hematoxylin and eosin and PAS staining. Original magnification: 100☐, scale bar: 50 µm. Quantification of lung histopathology (n = 6 per group). Data are representative of two independent experiments. Data are representative of two independent experiments and expressed as mean ± SEM. P-values were calculated using Student's t-test and one-way ANOVA post hoc test with Tukey's multiple comparison test. *P < 0.05, **P < 0.01, ***P < 0.001.

273x211mm (300 x 300 DPI)

AJRCMB Articles in Press. Published October 10, 2022 as 10.1165/rcmb.2022-0109OC

**Figure 7.** Anti-CD109 monoclonal antibody ameliorated AHR and eosinophilic airway inflammation during allergen sensitization and allergen challenge.

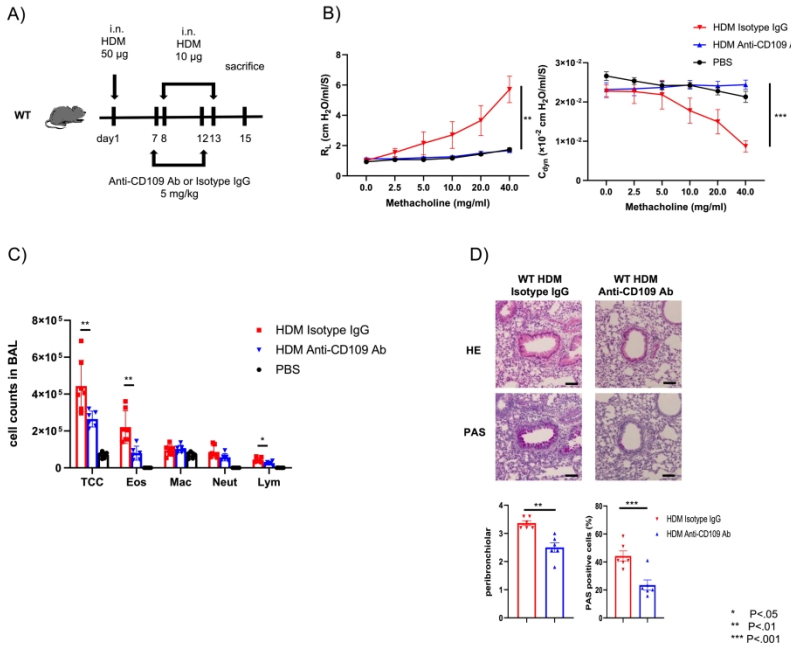


Figure 7. Anti-CD109 monoclonal antibody ameliorated AHR and eosinophilic airway inflammation during allergen sensitization and allergen challenge.
(A) Experimental timeline. WT mice were immunized as described in Fig 1A. Anti-CD109 monoclonal antibody or isotype IgG were intranasally administered on day7,12 before the house dust mite (HDM) challenge. (B) Lung resistance (RL) and dynamic compliance (Cdyn), (n = 6–7 per group). (C) Differential cell counts in BAL (n = 6–7 per group). TCC, total cell count; Eos, eosinophils. (D). Hematoxylin and eosin and PAS staining. Original magnification: 100□, scale bar: 50 μm. Quantification of lung histopathology (n = 6 per group). Data are representative of two independent experiments and expressed as mean ± SEM. P-values were calculated using Student's t-test and one-way ANOVA post hoc test with Tukey's multiple comparison test. *P < 0.05, **P < 0.01, ***P < 0.001.

295x211mm (300 x 300 DPI)

AJRCMB Articles in Press. Published October 10, 2022 as 10.1165/rcmb.2022-0109OC

# CD109 on dendritic cells regulates airway hyperreactivity and eosinophilic airway inflammation

Yuya Aono, MD, Yuzo Suzuki, MD, PhD, Ryo Horiguchi, PhD, Yusuke Inoue, MD, PhD, Masato Karayama, MD, PhD, Hironao Hozumi, MD, PhD, Kazuki Furuhashi, MD, PhD, Noriyuki Enomoto, MD, PhD, Tomoyuki Fujisawa, MD, PhD, Yutaro Nakamura, MD, PhD, Naoki Inui, MD, PhD, Shinji Mii, MD, PhD, Masahide Takahashi, MD, PhD, Takafumi Suda, MD, PhD

**ONLINE DATA SUPPLEMENT**

AJRCMB Articles in Press. Published October 10, 2022 as 10.1165/rcmb.2022-0109OC

## METHODS

### *Mice*

Female C57BL/6 mice (8 to 10-weeks-old) and OVA-specific T cell receptor (TCR) transgenic mice (OT-II) were purchased from Nippon SLC (Japan SLC, Inc., Shizuoka, Japan) and the Center for Animal Resources and Development, Kumamoto University (Kumamoto, Japan). *CD109*$^{-/-}$ mice were generated as previously described. [1] *CD109*$^{-/-}$ mice and OT-II mice were bred in our facility at Hamamatsu University School of Medicine using protocols approved by the Institutional Animal Care and Use Committee (29-045).

### *AHR induction and measurement of airway hyperresponsiveness*

Mice were intranasally (i.n.) sensitized with 50 μg HDM (*Dermatophagoides. pteronyssinus*; Greer Laboratories, XPB82D3A2.5) on Day 1, followed by 10 μg HDM (i.n.) on Days 8 and 13. In the experiment of **Fig. 6, Fig. 7,** and **Fig. S6**, mice were treated with neutralizing monoclonal anti-mouse CD109 antibody (i.n., 100 μg/mouse, anti-CD109 antibody, clone 4A13; Abmart) or IgG isotype controls (Fujifilm, Tokyo, Japan, 140-09511). An anti-mouse CD109 antibody was designed and prepared from mice by Abmart Inc. (Berkeley Heights, NJ). In the OVA model, mice were intraperitoneally immunized with OVA (50 μg, Sigma-Aldrich, St Louis, MO) and Alum (2 mg, Thermo Fischer Scientific, Rockford, IL) on days 1 and 8, and subsequently intranasally challenged with 50 μg OVA on days 19 to 21. In the experiment of **Fig. 3F**, Alexa Fluor 647-labeled OVA (Thermo Fisher Scientific) was intranasally administered in the last challenge to assess capability of antigen-uptake and -presentation of DCs.

Two days after the last HDM challenge or one day after the last OVA challenge, mice were anesthetized using a 300 μl intraperitoneal injection of ketamine (10 mg/ml) and xylazine (1

AJRCMB Articles in Press. Published October 10, 2022 as 10.1165/rcmb.2022-0109OC

mg/ml). Airway resistance and dynamic compliance measurements were conducted using the Fine Pointe RC system (Buxco Electronics, Inc., Wilmington, NC), in which mice were mechanically ventilated using a modified version as previously described. [2-4] Mice were sequentially challenged with aerosolized PBS (baseline), followed by increasing doses of methacholine (2.5 mg/ml, 5.0 mg/ml, 10 mg/ml, 20 mg/ml, and 40 mg/ml), Sigma-Aldrich, A2251. $R_L$ and $C_{dyn}$ values were recorded during a 3-min period after each methacholine challenge.

***Collection of bronchoalveolar lavage (BAL), serum, lung histology, and lung lysates***

After measuring AHR, BAL cells were obtained as previously described. [2-4] Lung histological sections and lung lysates were obtained and quantified. In some experiments, the lungs were stored in an RNA stabilization reagent (Qiagen, Valencia, CA).

After AHR measurements, the trachea was cannulated, and the lung was lavaged three times with 1 ml PBS to collect BAL cells. Blood was collected directly by cardiac puncture and serum was collected after centrifugation. Serum concentrations of total IgE (abcam, Cambridge, UK), HDM-specific IgE (Chondrex, Redmond, WA) and IgG1 (Abcam, Cambridge, UK) were measured by ELISA, according to the manufacturer's instructions.

Transcardial perfusion of the lungs was performed with cold PBS. Subsequently, the lungs were fixed and harvested for histology with 4% paraformaldehyde buffered in PBS. After fixation, the lungs were embedded in paraffin, cut into 4 μm sections, and stained with hematoxylin and eosin (H&E) and PAS.

According to a previous study, an inflammation score was assigned in a blinded fashion. [5] The

AJRCMB Articles in Press. Published October 10, 2022 as 10.1165/rcmb.2022-0109OC

peribronchiolar inflammation score from H&E staining was determined as 0, normal; 1, few cells; 2, a ring of inflammatory cells, one cell layer deep; 3, a ring of inflammatory cells, 2–4 cells deep; and 4, a ring of inflammatory cells more than four cells deep. PAS staining was performed by examining at least 20 consecutive fields. Numerical scores for the abundance of PAS-positive goblet cells in each airway were counted and expressed as a percentage of the total number of epithelial cells in that airway.

***Preparation of lung DC subsets***

The lungs were digested with collagenase (Roche, Basel, Switzerland) and DNase (Roche) using a GentleMACS™ dissociator (Miltenyi Biotec, North Rhine-Westphalia, Germany), and a single-cell suspension was prepared. The cells were incubated with anti-mouse CD11c-coated magnetic beads (Miltenyi Biotec) positively sorted by magnetic cell sorting (Miltenyi Biotec). For DC sorting, the following antibodies were used: peridinin-chlorophyll-protein complex-Cy5.5 (PerCP-Cy5.5)-labeled lineage marker (CD3e (clone 17A2, BioLegend, San Diego, CA), NK1.1 (clone PK136, BioLegend), CD19 (clone 6D5, BioLegend), CD45R (clone RA-3-6B2), PE-Cy7-labeled CD64 (clone X54-5/7.1, BioLegend), allophycocyanin-Cy7 (APC-Cy7)-labeled F4/80 (clone BM8, BioLegend), Alexa Flour 700-labeled anti-I-A/I-E (clone M5/114.15.2, BioLegend), Brilliant Violet 510-labeled anti-CD45 (clone 30-F11, BioLegend), FITC-labeled anti-CD11c (clone N418, BioLegend), PE-labeled XCR1 (clone ZET, BioLegend), and APC-labeled CD172a (clone P84, BioLegend). DCs were sorted using MoFlo Astrios EQ (Beckman Coulter, La Brea, CA). The sorted DC populations were routinely greater than 95% positive for the surface marker of interest.

AJRCMB Articles in Press. Published October 10, 2022 as 10.1165/rcmb.2022-0109OC

***In vitro coculture of lung DC subset and CD4$^+$ T cells***

Naïve CD4$^+$ T cells were obtained from OT-II murine spleen using the mouse CD4$^+$ T Cell Isolation Kit (Miltenyi Biotec). Purified CD4$^+$ T cells ($2 \times 10^5$/ml) were cocultured with lung DC subsets ($2 \times 10^4$/ml) for 7 days in the presence of 10 μg/ml $OVA_{323-339}$ peptide (Invitrogen). IL-2, IL-6, IL-10, IL-13, IL-17A, TNF-α, and IFN-γ levels in DCs-T cell coculture supernatants were measured by cytometric beads array (BD Biosciences, San Jose, CA) according to the manufacturer´s instructions. Brilliant Violet 421 labeled Annexin V (BioLegend) and Propidium Iodide Solution (BioLegend) were used for apoptosis assay of cocultured CD4$^+$ T cells on days 7. CellTrace violet (Thermo Fisher Scientific) was used for evaluating proliferation of cocultured CD4$^+$ T cells on days 3.

**Identification of lung ILC2s and Th2 cells**

Lung ILC2s cells were identified as live cells lacking the classical lineage markers (CD3, CD45R, Gr-1, CD11c, CD11b, Ter119, NK1.1, TCR-β, TCR-γδ, and FCεRIα), CD45$^+$ CD127$^+$ and ST2$^+$ cells, while lung Th2 cells were defined as IL5-producing CD4$^+$ T cells (IL-5$^+$ live CD45$^+$ CD3$^+$ CD4$^+$ cells) or IL13-producing CD4$^+$ T cells (IL-13$^+$ live CD45$^+$ CD3$^+$ CD4$^+$ cells).

***Preparation of bone marrow-derived DCs and adoptive transfers***

BM cells were harvested from femurs and tibias. BM cells were cultured at $4 \times 10^5$ cells/ml in RPMI 1640 supplemented with 10% fetal calf serum (FCS), 1000 U/ml recombinant murine GM-CSF (R&D), and 400 U/ml recombinant murine IL-4 (R&D). On day 8, cells were harvested and incubated with HDM (20 μg/ml) for 6 hours. BMDCs ($2.0 \times 10^5$) were adoptively transferred intravenously into C57BL/6 mice (day 1) challenged intratracheally with $2.0 \times 10^5$

AJRCMB Articles in Press. Published October 10, 2022 as 10.1165/rcmb.2022-0109OC

BMDCs or HDM (10μg/mouse) on days 8 and 13 and sacrificed on day 15.

***Flow cytometry analysis of BAL fluids, ILC2s, Th2 cells, cell surface, and intracellular staining***

BAL cells were stained with surface phycoerythrin (PE)-labeled anti-Singlec-F (clone E50-2440, BD Pharmingen, San Diego), APC-labeled anti-Ly-6G/Ly-6C (clone RB6-8C5, BioLegend), PE-Cy (PE-Cy7)-labeled anti-CD45 (clone 30-F11, BioLegend), APC-Cy7-labeled anti-CD11c (clone N418, BioLegend), PerCP-Cy5.5-labeled anti-CD3e (clone17A2, BioLegend), FITC-labeled anti-CD19 (clone MB19-1, BioLegend), Pacific-blue labeled anti-CD11b (clone M1/70, BioLegend).

Lung ILC2s cells were identified as live cells lacking the classical lineage markers (CD3, CD45R, Gr-1, CD11c, CD11b, Ter119, NK1.1, TCR-β, TCR-γδ, and FCεRIα), $CD45^+$ $CD127^+$ $ST2^+$ cells, while lung Th2 cells were defined as IL5-producing $CD4^+$ T cells ($IL\text{-}5^+$ live $CD45^+$ $CD3^+$ $CD4^+$ cells) or IL13-producing $CD4^+$ T cells ($IL\text{-}13^+$ live $CD45^+$ $CD3^+$ $CD4^+$ cells). Following antibody were used: biotinylated anti-mouse lineage (CD3e (145-2C11; BioLegend), CD45R (RA3-6B2; BioLegend), Ly-6G/Ly-6C (RB6-8C5; BioLegend), CD11c (N418; BioLegend), CD11b (M1/70; BioLegend), Ter119 (TER-119; BioLegend), NK1.1 (PK136; BioLegend), TCR-β (H57-597; BioLegend), TCR-γδ (BioLegend), and FCER1A/FCεRIα (MAR-1; BioLegend), PerCP-Cy5.5-labeled anti-ST2 (clone DIH9, BioLegend), BV510-labeled anti-CD127 (clone A7R34, BioLegend), eFlour 450-labeled anti-CD45 (clone 30-F11, Thermo Fisher Scientific) , PerCP-Cy5.5-labeled anti-CD3 (clone 17A2, BioLegend), Pacific-blue labeled anti-CD4 (clone GK1.5, BioLegend), BV510-labeled anti-CD45 (clone 30-F11, BioLegend), PE-labeled anti-IL5 (clone TRFK5, BioLegend) and PECy7-labeled anti- IL-13 (clone eBio13A,

AJRCMB Articles in Press. Published October 10, 2022 as 10.1165/rcmb.2022-0109OC

Thermo Fisher Scientific).

The antibodies used for analyzing CD109 expressions in lung cells were: FITC-labeled anti-EpiCAM (clone G8.8, BioLegend), APC-labeled anti-CD31 (clone 390, BioLegend), PECy7-labeled anti-CD45 (clone 30-F11, Biolegend), BV510-labeled anti-CD45 (clone 30-F11, BioLegend) , FITC-labeled anti-CD11c (clone N418, BioLegend), APC-labeled anti-I-A/I-E (clone M5/114.15.2, BioLegend), APC-Cy7-labeled anti-F4/80 (clone BM8, BioLegend), Pacific-blue labeled anti-CD11b (clone M1/70, BioLegend), PE-Cy7-labeled anti-CD103 (clone 2E7, BioLegend), FITC- labeled anti-CD19 (clone MB19-1, BioLegend), PerCP-Cy5.5-labeled anti-CD3 (clone 17A2, BioLegend), APC-labeled anti-CD4 (clone RM4-5, BioLegend), BV510-labeled anti-CD45 (clone 30-F11, BioLegend), PerCP-Cy5.5-labeled anti-ST2 (clone DIH9, BioLegend), PECy7-labeled anti-CD127 (clone A7R34, BioLegend), BV510-labeled anti-CD45 (clone 30-F11, BioLegend), FITC-streptavidin (BioLegend), biotinylated anti-mouse lineage (CD3e (145-2C11; BioLegend), CD45R (RA3-6B2; BioLegend), Ly-6G/Ly-6C (RB6-8C5; BioLegend), CD11c (N418; BioLegend), CD11b (M1/70; BioLegend), Ter119 (TER-119; BioLegend), NK1.1 (PK136; BioLegend), TCR-β (H57-597; BioLegend), TCR-γδ (BioLegend), and FCER1A/FCεRIα (MAR-1; BioLegend). Expression intensity of CD109 was evaluated using the PE-labeled anti-CD109 (clone 496920, R&D).

The cell-surface $CD109^+$ DC and $CD109^-$ DC antibodies were: PE-Cy7-labeled anti-CD40 (clone 3/23, BioLegend), APC-labeled anti-CD86 (clone GL-1, BioLegend), Pacific-blue labeled anti-CD80 (clone 16-10A1, BioLegend), Biotin-labeled anti-ICOS-Ligand (clone HK5.3, BioLegend), Brilliant Violet 421-labeled anti-streptavidin (BioLegend), PECy7-labeled anti-PD-L2 (clone TY25, BioLegend), APC-labeled anti-PD-L1 (clone 10F.9G2, BioLegend). Intracellular staining was performed using PE-labeled anti-Runx3 (clone R3-5G4, BD

AJRCMB Articles in Press. Published October 10, 2022 as 10.1165/rcmb.2022-0109OC

Bioscience) and BD Cytofix/Cytoperm (BD Bioscience) or Alexa Fluor 647-labeled antiphospho Smad2 (pS465/pS467)/Smad3 (pS423/pS425) (clone O72-670, BD Bioscience), BD Cytofix™ Fixation Buffer, and BD Phosflow™ Perm Buffer III according to the manufacturer's instructions.

Flow cytometry was done with a Gallios Flow Cytometer (Beckman Coulter). Data were analyzed with FlowJo version 8.6 software (TreeStar, Ashland, OR).

***Reverse transcription-polymerase chain reaction (RT-PCR) assays***

L4, IL5, IL13, IL25, IL33, and TSLP expression in the lung lysate was measured by RT-PCR. Total RNA was extracted with RNAeasy mini (Qiagen, Valencia, CA). cDNA was prepared from RNA using the High-Capacity cDNA Reverse Transcription Kit (Applied Biosystems). RT-PCR was performed using StepOnePlus (Applied Biosystems). ΔΔCt was used for data analysis.[25] Each gene expression was normalized to the housekeeping gene GAPDH.
The specific RT-PCR primer pairs were: IL-4 (forward 5′- GGTCTCAACCCCCAGCTAGT,-3′ and reverse 5′- GCCGATGATCTCTCTCAAGTGAT-3′), IL-5 (forward 5′- CTCTGTTGACAAGCAATGAGACG -3′ and reverse 5′- TCTTCAGTATGTCTAGCCCCTG-3′), IL-13 (forward 5′- CCTGGCTCTTGCTTGCCTT -3′ and reverse 5′- GGTCTTGTGTGATGTTGCTCA -3′), IL-25 (forward 5′- ACAGGGACTTGAATCGGGTC -3′ and reverse 5′- TGGTAAAGTGGGACGGAGTTG -3′), IL-33 (forward 5′- TCCAACTCCAAGATTTCCCCG-3′ and reverse 5′- CATGCAGTAGACATGGCAGAA-3′), TSLP (forward 5′- ACGGATGGGGCTAACTTACAA-3′ and reverse 5′- AGTCCTCGATTTGCTCGAACT-3′) and GAPDH (forward 5′- AACTTTGGCATTGTGGAAGG-3′ and reverse 5′- GGATGCAGGGATGATGTTCT). The

AJRCMB Articles in Press. Published October 10, 2022 as 10.1165/rcmb.2022-0109OC

⊿⊿Ct method was used for data analysis.

***Reagents***

Cells were cultured in RPMI 1640 medium (Gibco BRL, Tokyo, Japan) supplemented with 3 mM L-glutamine (Sigma, St. Louis, MO), 1% penicillin-streptomycin (Gibco BRL), and 10% heat-inactivated FCS (Gibco BRL).

AJRCMB Articles in Press. Published October 10, 2022 as 10.1165/rcmb.2022-0109OC

## Supplementary Figure

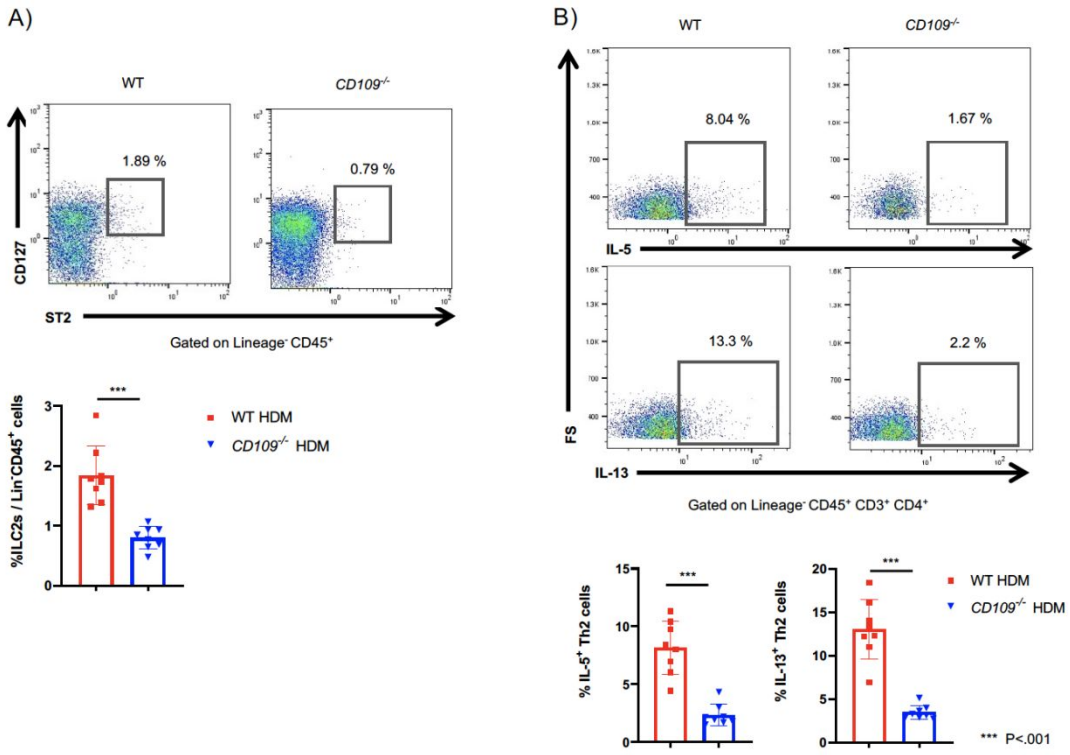


**Figure S1.** Reduced frequencies of ILC2s and Th2 cells in CD109-deficient mice.

*CD109*$^{-/-}$ mice and WT mice were immunized as described in **Fig 1A**. The frequencies of ILC2s (Lin$^{-}$ CD45$^{+}$ CD127$^{+}$ ST2$^{+}$) (n = 8 per group, **A**) and Th2 cells (IL5$^{+}$ CD3$^{+}$ CD4$^{+}$cells and IL13$^{+}$ CD3$^{+}$ CD4$^{+}$cells) (n = 8 per group, **B**) in lung were analyzed. Data are results from single experiment and expressed as mean ± SEM. P-values were calculated using Student's *t*-test and one-way ANOVA post hoc test with Tukey's multiple comparison test. *P < 0.05, **P < 0.01, ***P < 0.001.

AJRCMB Articles in Press. Published October 10, 2022 as 10.1165/rcmb.2022-0109OC

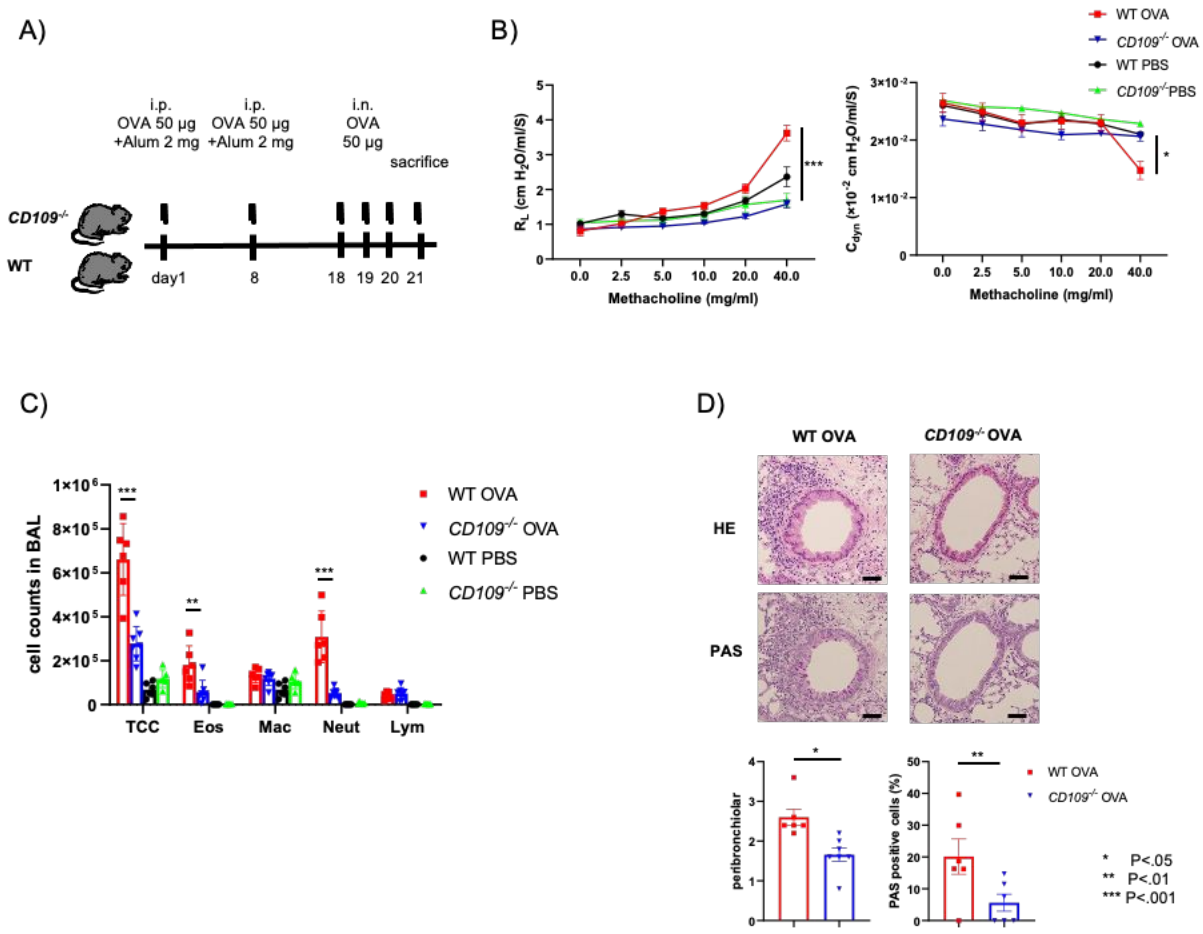


**Figure S2.** Airway hyperreactivity and eosinophilic airway inflammation in *CD109*$^{-/-}$ mice immunized with OVA + Alum.

(**A**) Experimental timeline. WT and CD109$^{-/-}$ mice were immunized with OVA + Alum. (**B**) Lung resistance ($R_L$) and dynamic compliance ($C_{dyn}$), (n = 6 per group). (**C**) Differential cell counts in BAL (n = 6 per group). TCC, total cell count; Eos, eosinophils. (**D**). Hematoxylin and eosin and PAS staining. Original magnification: 100×, scale bar: 50 µm. Quantification of lung histopathology (n = 6 per group). Data are representative of at least two independent experiments and expressed as mean ± SEM. P-values were calculated using Student's *t*-test and one-way ANOVA post hoc test with Tukey's multiple comparison test. *P < 0.05, **P < 0.01, ***P < 0.001.

AJRCMB Articles in Press. Published October 10, 2022 as 10.1165/rcmb.2022-0109OC

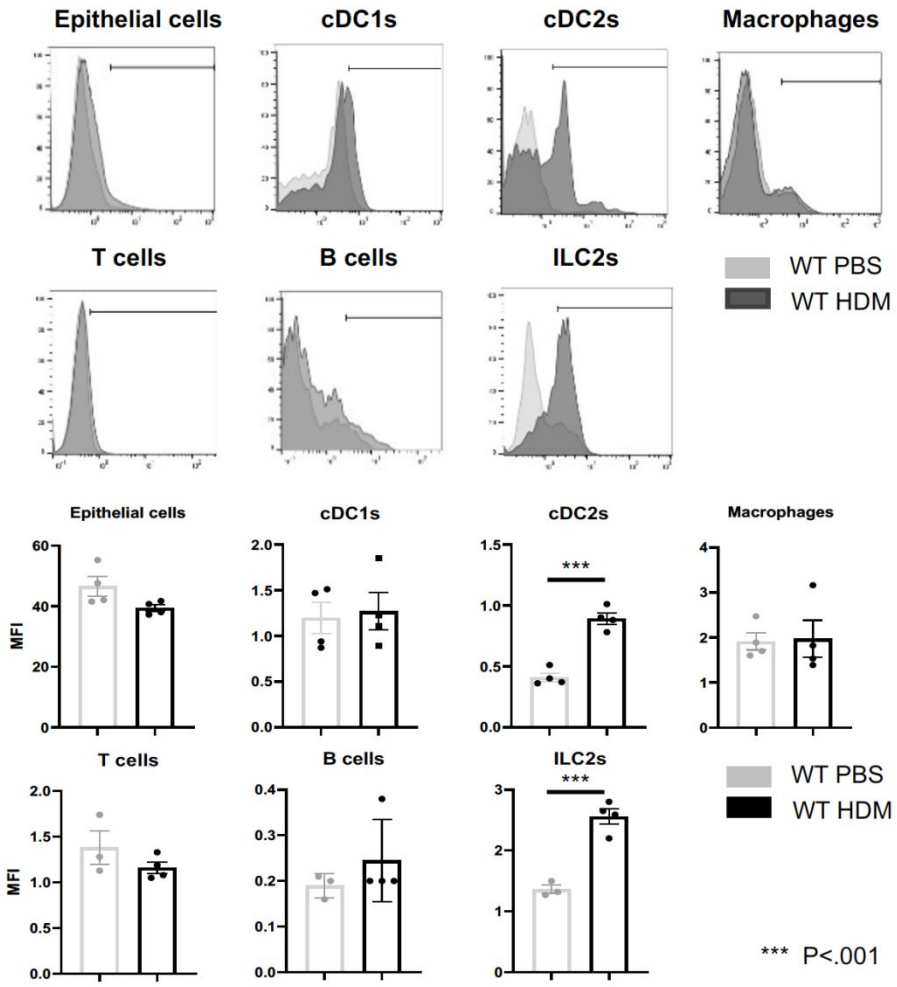


**Figure S3.** CD109 expression was inducible after allergen sensitization.

WT mice were intranasally (i.n.) sensitized (days 1) and challenged with house dust mite (HDM, days 8 and 13) as described in **Fig 1A**. Subsequently, CD109 expression in lung immune cells was analyzed on day 15. Representative FACS histogram and mean fluorescence intensity (MFI) of CD109 (n = 4 per group). Data are representative of two independent experiments and expressed as mean ± SEM. P-values were calculated using Student's *t*-test. ***P < 0.001.

AJRCMB Articles in Press. Published October 10, 2022 as 10.1165/rcmb.2022-0109OC

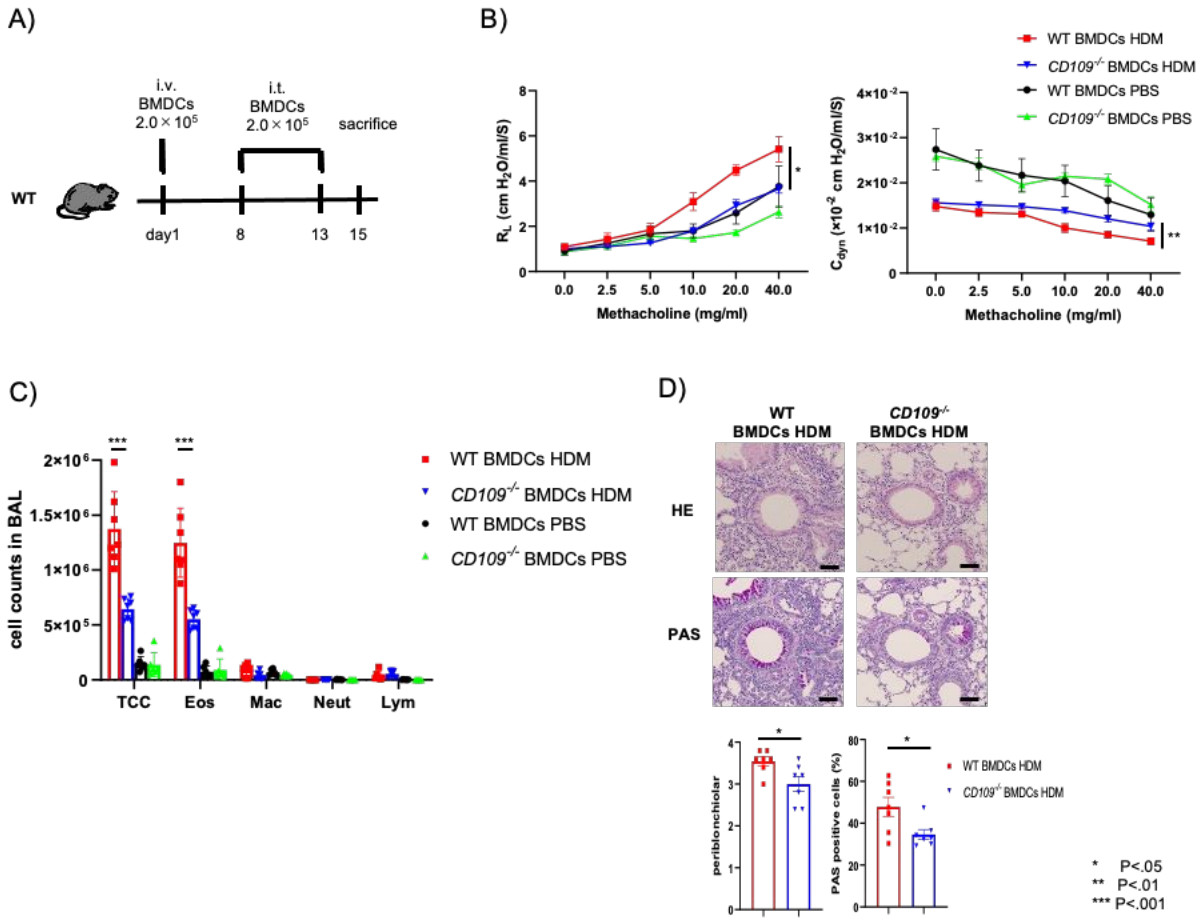


**Figure S4.** CD109 expression in DCs was responsible for the induction of asthmatic phenotype during allergen challenge.

(**A**) Experimental timeline. Cultured BMDCs from WT or *CD109*$^{-/-}$ mice were stimulated with house dust mite (HDM) for six hours and then intravenously injected into WT mice. Then mice were intratracheally challenged with HDM-stimulated BMDCs on days 8 and 13. (**B**) Lung resistance ($R_L$) and dynamic compliance ($C_{dyn}$), (n = 6–7 per group). (**C**) Differential cell counts in BAL (n = 7 per group). TCC, total cell count; Eos, eosinophils. (**D**). Hematoxylin and eosin and PAS staining. Original magnification: 100×, scale bar: 50 μm. Quantifications of lung histopathology (n = 7 per group). Data are representative of two independent experiments and

AJRCMB Articles in Press. Published October 10, 2022 as 10.1165/rcmb.2022-0109OC

expressed as mean ± SEM. P-values were calculated using Student's *t*-test and one-way ANOVA post hoc test with Tukey's multiple comparison test. *P < 0.05, **P < 0.01.

AJRCMB Articles in Press. Published October 10, 2022 as 10.1165/rcmb.2022-0109OC

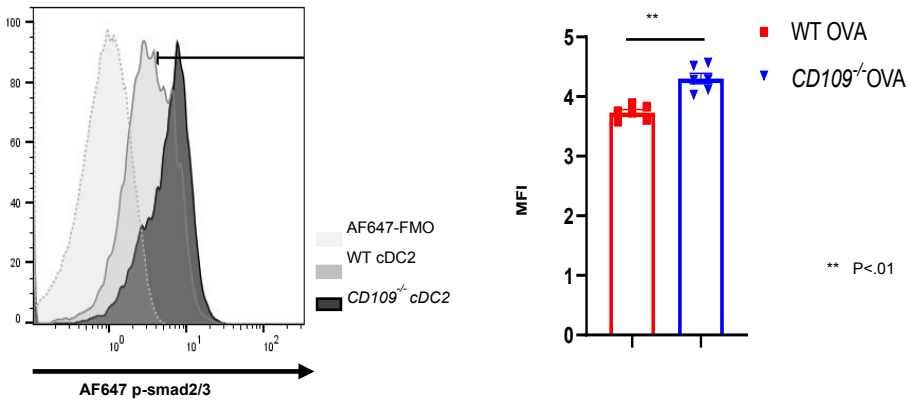


**Figure S5.** The expression of phosphorylated SMAD2/3 in lung-cDC2s immunized with OVA. WT and *CD109*$^{-/-}$ mice were immunized with OVA + Alum as described in **Fig S1A**. Representative FACS histogram and mean fluorescence intensity (MFI) of SMAD2/3 phosphorylation in lung-cDC2s are shown (n = 6). Data are representative of two independent experiments and expressed as mean ± SEM. P-values were calculated using Student's *t*-test. **P < 0.01.

AJRCMB Articles in Press. Published October 10, 2022 as 10.1165/rcmb.2022-0109OC

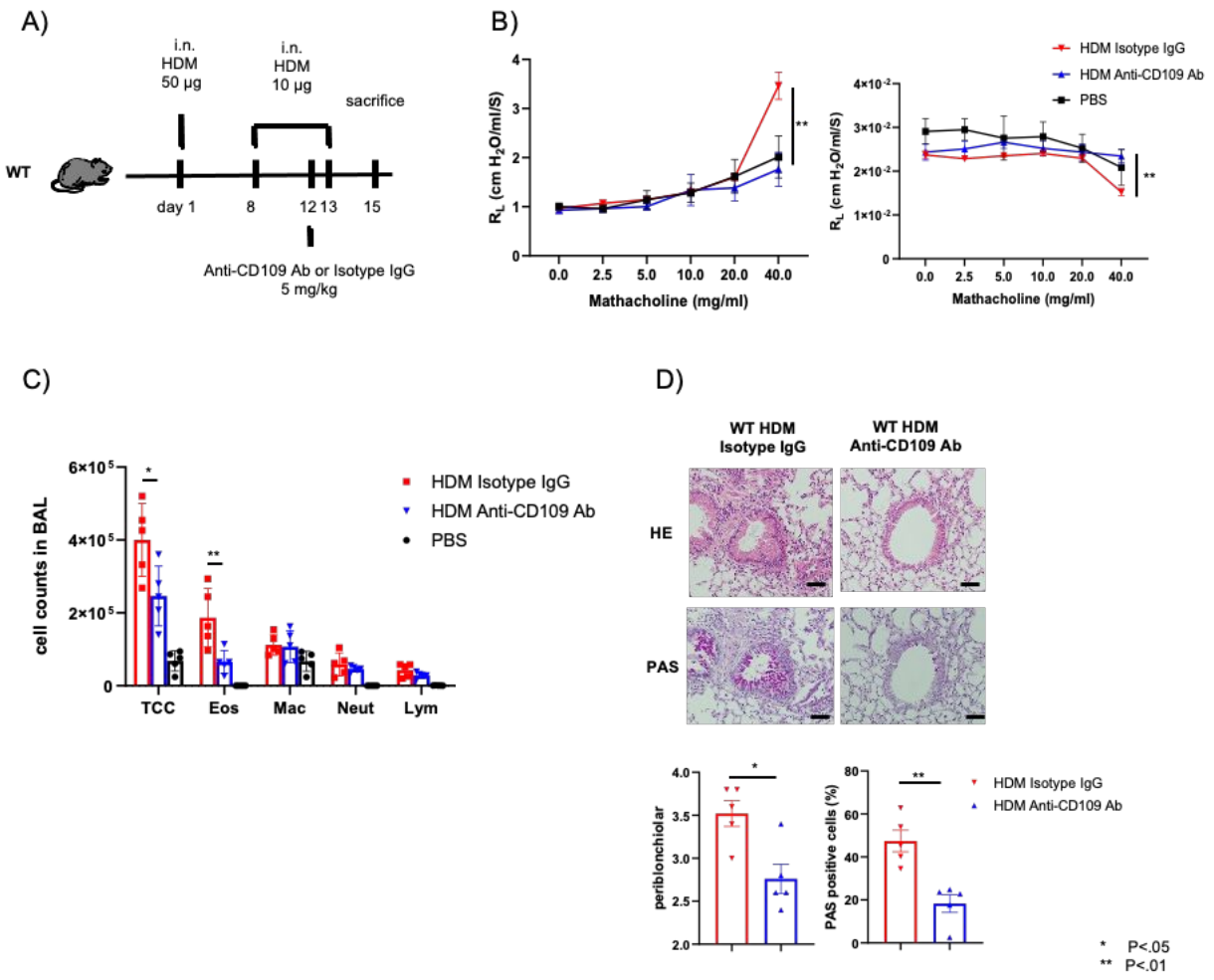


**Figure S6.** Anti-CD109 monoclonal antibody ameliorated AHR and eosinophilic airway inflammation in HDM-challenged mice.

(**A**) Experimental timeline. WT mice were immunized as described in **Fig 1A**. Anti-CD109 monoclonal antibody or isotype IgG were intranasally administered before the last house dust mite (HDM) challenge (day12). (**B**) Lung resistance ($R_L$) and dynamic compliance ($C_{dyn}$), (n =5 per group). (**C**) Differential cell counts in BAL (n = 5 per group). TCC, total cell count; Eos, eosinophils. (**D**). Hematoxylin and eosin and PAS staining. Original magnification: 100×, scale

AJRCMB Articles in Press. Published October 10, 2022 as 10.1165/rcmb.2022-0109OC

bar: 50 μm. Quantification of lung histopathology (n = 5 per group). Data are representative of two independent experiments and expressed as mean ± SEM. P-values were calculated using Student's *t*-test and one-way ANOVA post hoc test with Tukey's multiple comparison test. *P < 0.05, **P < 0.01, ***P < 0.001.


1. Mii S, Murakumo Y, Asai N, Jijiwa M, Hagiwara S, Kato T, et al. Epidermal hyperplasia and appendage abnormalities in mice lacking CD109. Am J Pathol 2012; 181:1180-9.
2. Galle-Treger L, Suzuki Y, Patel N, Sankaranarayanan I, Aron JL, Maazi H, et al. Nicotinic acetylcholine receptor agonist attenuates ILC2-dependent airway hyperreactivity. Nat Commun 2016; 7:13202.
3. Suzuki Y, Maazi H, Sankaranarayanan I, Lam J, Khoo B, Soroosh P, et al. Lack of autophagy induces steroid-resistant airway inflammation. J Allergy Clin Immunol 2016; 137:1382-9.e9.
4. Suzuki Y, Aono Y, Akiyama N, Horiike Y, Naoi H, Horiguchi R, et al. Involvement of autophagy in exacerbation of eosinophilic airway inflammation in a murine model of obese asthma. Autophagy.
5. Tong J, Bandulwala HS, Clay BS, Anders RA, Shilling RA, Balachandran DD, et al. Fas-positive T cells regulate the resolution of airway inflammation in a murine model of asthma. J Exp Med 2006; 203:1173-84.


AJRCMB Articles in Press. Published October 10, 2022 as 10.1165/rcmb.2022-0109OC